

20000831230

ARO 26163.1-MS-A

AD-A244 472



(2) ✓

DEVELOPMENT, FABRICATION

AND

BALLISTIC TESTING

OF

NEW, NOVEL LOW-COST

HIGH PERFORMANCE

BALLISTIC MATERIALS

DTIC
FLECTE
JAN 08 1992
S D

Final Report

Contract No. DAAL01-83-C-0032

Richard J. Palicka

Jack A. Rubin

This document has been approved
for public release and sale; its
distribution is unlimited.

July 1991

92-00503



Reproduced From
Best Available Copy

MASTER COPY

KEEP THIS COPY FOR REPRODUCTION PURPOSES

REPORT DOCUMENTATION PAGE

Form Approved

OMB No. 3704-0188

Public reporting burden for this collection of information is estimated to average 1 hour per response, including the time for reviewing instructions, searching existing data sources, gathering and maintaining the data needed, and completing and reviewing the collection of information. Send comments regarding this burden estimate or any other aspect of this collection of information, including suggestions for reducing the burden, to Washington Headquarters Services, Directorate for Information Operations and Reports, 1215 Jefferson Davis Highway, Suite 1204 Arlington, VA 22202-4302, and to the Office of Management and Budget, Paperwork Reduction Project (3704-0188), Washington, DC 20503.

1. AGENCY USE ONLY (Leave blank)		2. REPORT DATE Oct 91	3. REPORT TYPE AND DATES COVERED Final Report - 1 Oct 88 - 30 Sep 90
4. TITLE AND SUBTITLE Development Fabrication and Ballistic Testing of New, Novel Low Cost High Performance Ballistic Materials			5. FUNDING NUMBERS DAAL03-88-C-0032
6. AUTHOR(S) Richard Palicka Jack Rubin			
7. PERFORMING ORGANIZATION NAME(S) AND ADDRESS(ES) Cercom Inc. 1960 Watson Way Vista, CA 92083			8. PERFORMING ORGANIZATION REPORT NUMBER
9. SPONSORING / MONITORING AGENCY NAME(S) AND ADDRESS(ES) U. S. Army Research Office P. O. Box 12211 Research Triangle Park, NC 27709-2211			10. SPONSORING / MONITORING AGENCY REPORT NUMBER ARO 26165.1-MS-
11. SUPPLEMENTARY NOTES The view, opinions and/or findings contained in this report are those of the author(s) and should not be construed as an official Department of the Army position, policy, or decision, unless so designated by other documentation.			
12a. DISTRIBUTION / AVAILABILITY STATEMENT Approved for public release; distribution unlimited.			12b. DISTRIBUTION CODE
13. ABSTRACT (Maximum 200 words) The Program goal was to develop improved low cost high performance ballistic armor ceramic materials thru microstructural control. The system $Al_2O_3 +$ SiC particulates was investigated by varying the type, purity and particle sizes of the starting material and the volume percentages of the SiC dispersed phase. Low cost as well as high cost starting materials were investigated. Physical, mechanical and microstructural data was obtained. The study determined that low cost starting materials appear to work as well as high cost materials and that an inexpensive Al_2O_3 -SiC composite containing only 10 v/o SiC could perform as well as sintered alpha silicon carbide as a ceramic ballistic armor.			
14. SUBJECT TERMS Ceramic Armor Materials - Alumina, Silicon Carbide Composites			15. NUMBER OF PAGES 58
			16. PRICE CODE
17. SECURITY CLASSIFICATION OF REPORT UNCLASSIFIED	18. SECURITY CLASSIFICATION OF THIS PAGE UNCLASSIFIED	19. SECURITY CLASSIFICATION OF ABSTRACT UNCLASSIFIED	20. LIMITATION OF ABSTRACT UL

TABLE OF CONTENTS

	Page
1.0 INTRODUCTION	1
2.0 EXPERIMENTAL PROCEDURES	1
2.1 RAW MATERIALS	1
2.2 POWDER PREPARATION	2
2.3 FORMING	2
3.0 PROPERTY MEASUREMENTS	2
3.1 DENSITY	2
3.2 STRENGTH	2
3.3 HARDNESS	3
3.4 FRACTURE TOUGHNESS	3
3.5 GRAIN SIZE	3
4.0 RESULTS	3
5.0 DISCUSSION	5
6.0 CONCLUSIONS	10
7.0 REFERENCES	11

TABLES

FIGURES

APPENDICES

APPENDIX I.

APPENDIX II.

Accession For	
NTIS CRA&I	<input checked="" type="checkbox"/>
DTIC TAB	<input type="checkbox"/>
Unannounced	<input type="checkbox"/>
Justification	
By	
Distribution	
Availability Codes	
Avail and/or	Special
A-1	

LIST OF TABLES

	Title	Page
Table 1	Raw Materials	12
Table 2.	Residual Penetrations and Penetration Reductions for Impacts at 1500 m/s on Cercom Incorporated Samples	13
Table 3.	Comparison of Scaled Penetration Reductions of Baseline AD90 and Cercom Incorporated Ceramics	14

LIST OF FIGURES

	Title	Page
Figure 1.	Effect of Pressure Assisted Densification (PAD) on the strength and grain size of "pure" alumina.	15
Figure 2.	Effect of $V\%$ SiC on the strength of hot pressed alumina.	16
Figure 3.	Effect of Volume % SiC on the strength of composites Pressure Assisted Densified (PAD) at 1750°.	17
Figure 4.	Relationship between Weibull modulus (m) and standard deviation (σ) of strength measurement (MOR-4 pt).	18
Figure 5.	Effect of $V\%$ SiC on the hardness of Al_2O_3 -SiC composites.	19
Figure 6.	Aluminum Oxide comparisons.	20
Figure 7.	Al_2O_3 -SiC composites performance.	21
Figure 8.	Idealized microstructures in the system Al_2O_3 -SiC.	22
Figure 9.	Morphology of alumina grain.	23
Figure 10.	Idealized microstructures and direction of residual stresses.	24
Figure 11.	Schematic of microstructural features in materials.	25
Figure 12.	Development of microstructures in Al_2O_3 -SiC composites.	26

LIST OF FIGURES - Cont'd

Title	Page
Figure 13. Effect of grain size on the strength of "pure" hot pressed alumina.	27
Figure 14. Effect of average grain size on the strength of alumina ceramics (with or without SiC).	28
Figure 15. True histograms of strength distribution of two samples of 50 % Al_2O_3 - 50 % SiC (Alcoa A-16 SG - Lonza 15-UF) - singularly and then combined.	29
Figure 16. Schematic histograms of strength distributions.	30
Figure 17. Al_2O_3 -SiC composite with unusually high Weibull modulus.	31
Figure 18. Retained strength after compressive failure of a constrained ceramic target.	32

1.0 INTRODUCTION

Sintered alumina (Al_2O_3) ceramic, e.g., Coors AD90, is a standard ballistic armor material. Sintered alpha silicon carbide (SiC) ceramic, however, performs much better than Al_2O_3 . It was speculated that, perhaps, by dispersing inexpensive silicon carbide particles in an inexpensive alumina matrix, a ceramic alloy or composite might be produced that performed as good as essentially-pure SiC , but at a lower cost. It was also thought that it would be useful to investigate the difference between more expensive beta- and very finely ground alpha-silicon carbides and the less expensive standard "abrasive grades" as the dispersed phase. It was also thought that it would prove interesting to study the differences produced between more expensive, high purity alumina powder and the standard, ceramic grade alumina powder to produce the Al_2O_3 matrix.

If Al_2O_3 - SiC (particulate) ceramics could be produced with physical, mechanical, and microstructural properties that suggested good potential ballistic performance, then ballistic tests would be performed on materials derived from this program.

This program, "Development, Fabrication, and Ballistic Testing of New, Novel, Low Cost, High Performance Ballistic Materials" was initiated to test this hypothesis.

2.0 EXPERIMENTAL PROCEDURES

2.1 RAW MATERIALS

Readily available commercial Al_2O_3 and SiC powders (See Table 1) were used throughout this study. Ceralox, grade HPA, (99.97% pure plus 0.5 % MgO), with an average particle size of 0.5 microns and a surface area of 10.8 m^2/g at a cost of \$4.80 per pound is considered the "high cost" alumina. ALCOA A-16 SG, with an average particle size of 0.45 microns and a surface area of 8.7 m^2/g at a cost of approximately \$1.28 per pound, is considered the "low cost" alumina. Three grades of commercially available SiC powders were used throughout this study. H. C. Starck Grade B-10 beta-silicon carbide, having an average particle size of 0.4 microns at a cost of \$10.50 per pound was considered the "high cost" silicon carbide. As a comparison, an expensive (\$9.00 per pound) finely divided, alpha-silicon carbide, Lonza Grade 15-UF, having an average particle size of 0.8 microns was introduced for comparison of the effect of alpha- vs. beta- SiC . Lonza F-1000, "abrasive grade" alpha silicon carbide, at a cost of \$3.60 per pound, was considered the "low cost" silicon carbide.

2.2 POWDER PREPARATION

A milling operation was used to prepare the various blends of Al_2O_3 and SiC . (It should be noted, however, that the milling operation was used to assure a uniform dispersion of the constituents, and not to commutate the materials.) The starting materials were weighed out and placed in a Nalgene plastic jar mill containing 1/2 inch diameter, high purity alumina rod grinding media. Isopropyl alcohol was used as the milling fluid. The powders were "mixed" for eight (8) hours and then dried for 24 hours at 75°C . The powder was "dry milled" for eight (8) hours to break up any agglomerates.

2.3 FORMING

The milled powders were carefully loaded into GrafoilTM - lined graphite dies. The graphite tooling was designed to produce a part 6" x 6" and the powder charges were adjusted (by calculating from the assumed theoretical density of each composition) to form plates about 3/8" thick. The loaded die was then placed in an inductively heated furnace and sintered using Cercom's PAD (Pressure Assisted Densification) process. The pressure used was 3000 psi (approximately 21 MPa), and temperature varied from 1600°C to 1825°C , depending on the predetermined conditions for each run. The sintered, densified ceramic part was removed from the graphite tooling and its surfaces were "grit blasted" to remove any residual GrafoilTM.

3.0 PROPERTY MEASUREMENTS

3.1 DENSITY

The theoretical densities for the Al_2O_3 - SiC composites were calculated using the rule of mixtures. Individual densities were determined on the "as pressed" billets by the water immersion technique. The determined densities were corrected for water temperature.

3.2 STRENGTH

Modulus of rupture values were obtained from 10 - 15 specimens using the 4-point method as described in Military Specification MS 1942A. The Weibull number was obtained from the distribution of values obtained from the MOR test.

3.3 HARDNESS

Hardness values reported are an average of five readings obtained using a Knoop diamond pyramid indenter at 1 Kg load.

3.4 FRACTURE TOUGHNESS

The fracture toughness values were determined using a Vickers indenter. The load was 10 Kg. Values reported are the average of five values.

3.5 GRAIN SIZE

The grain size was determined by the Linear intercept method.

4.0 RESULTS:

The results for all of the runs made in this investigation of silicon carbide (SiC), particulate reinforced, alumina ceramic-matrix-composites are shown in Appendix I along with two Cercom proprietary, "baseline" aluminas, Ebon A and Ebon AZC, as well as one Cercom proprietary "baseline" silicon carbide, PAD SiC Type B. In this appendix results are given for:

- Composition
- PAD¹ Temperature
- Density
 - Actual
 - Theoretical
- Grain Size
- Fracture Toughness
- Strength [Modulus of Rupture (MOR)]
- Weibull modulus

¹ PAD = Pressure Assisted Densification

In most cases where there is the absence of some data in this tabulation (Appendix I), the sample produced in the "run" was of a density below 97.5% of its theoretical value and was not, therefore, intended for ballistic testing. In other cases where the density was greater than 97.5% of its theoretical value but data is missing, the lack of time, funding, or both precluded the measurement from being made.

The strengths and grain sizes of pure Al_2O_3 achieved in this study as a function of PAD temperature are shown in Figure 1. Figure 2 shows the strengths as a function of volume per cent (V/o) silicon carbide (SiC) in various alumina (Al_2O_3) ceramic matrices. Figure 3 is a similar plot, but only looks at data from the runs at 1750°C. Figure 4 shows the relationship between Weibull modulus (m) and the standard deviation [std. dev (σ)] of the strength [Modulus of Rupture (MOR)]. Figure 5 illustrates the unusual relationship between hardness and V/o SiC in the Cercom proprietary alumina matrix, Ebon AZC, compared with the more conventional alumina matrices, Alcoa A-16 SG, Ceralox, and Ebon A (proprietary).

Microstructures of the majority of the Al_2O_3 -SiC ceramic produced in each of the runs are shown in Appendix II. Most of the photos are based on SEM fractographs. The rest of the photos are based on polished and etched cross-sections (optical micrographs).

Lack of funding and time limited the amount of ballistic data obtained in this study. Figure 6 shows the ballistic performance of three proprietary Cercom alumina (matrices) ceramics compared: Ebon A, Ebon AZ and Ebon AZC against Coors AD90 as a "baseline". Figure 7 illustrates the outstanding ballistic performance of two Al_2O_3 -SiC ceramic matrix composites derived from this study. Composition "A" is 10 V/o SiC dispersed in Cercom's proprietary alumina matrix Ebon AZC. Composition "B" is 10 V/o SiC dispersed in Cercom's proprietary alumina matrix Ebon A. The top-performing Cercom SiC also shown on this chart is Cercom's proprietary PAD SiC Type B. The alumina baseline material shown on this graph is Coors AD90, while the silicon carbide (SiC) baseline material is Carborundum [British Petroleum (BP)] sintered alpha silicon carbide (Hexaloy). [Note: The baseline silicon carbide is shown in the legend of this chart as Sohio (Standard Oil of Ohio) SiC. This is its former designation prior to the acquisition of the USA company by the UK company.]

In addition, data for Cercom's Ebon A and PAD SiC Type B, considered as "reference test", was obtained at Southwest Research Institute. The data is presented in Tables II and III.

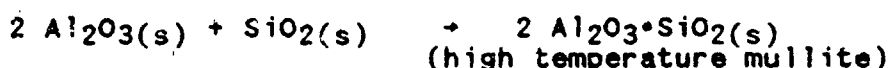
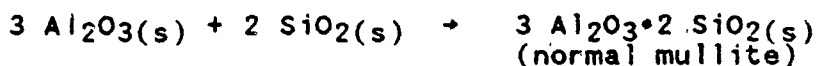
5.0 DISCUSSION

The interpretation of the data for the ceramic system alumina (Al_2O_3) - silicon carbide (SiC) particulates is very complex. Many variables are interacting simultaneously to produce the results obtained in this study.

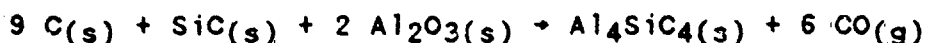
The most interesting effect is the location and distribution of the dispersed, second-phase - in this case, particulates of SiC . Since it is extremely difficult to perform exact microstructural analyses on this system, a schematic diagram of the potential microstructures achievable are shown in Figure 8. These sketches show that there are at least four probable microstructures, i.e., (i) all of the silicon carbide particles located within the alumina grains; (ii) all of the silicon carbide located at the three-grain intersections (i.e., "triple-points") of the alumina grains; (iii) all of the silicon carbide grains located along the alumina grain boundaries including the "triple-points"; and (iv) the silicon carbide grains are located within the alumina grains and along the alumina grain boundaries as well as at the "triple points" of the alumina grains. Of course the grain size, shape and distribution of the alumina ceramic matrix will change according to the processing (i.e., fabrication) conditions, the starting type of alumina, and its chemistry, as well as its interaction, if any, with the silicon carbide grains. The morphology of a typical single crystal grain of Al_2O_3 (hexagonal, rhombohedral) is shown in Figure 9. Because of the platelike, anisotropic nature of the grains, the grain structure in fractured and polished sections can appear to vary from equiaxed hexagonal grains to needle-like acicular grains which may indeed be the same grain, but viewed from different angles, as also shown in the schematic cross-sections in Figure 9. The silicon carbide grains are normally also hexagonal regardless as to whether they start out as cubic or hexagonal powder. The morphology, however, of the hexagonal SiC powder is normally a jagged fragment as it is the product of a crushed, Acheson process grain. On the other hand, the beta SiC starting powder is more regular in outline because it is the product of a chemical process.

[Note: In the following discussion of the potential chemical reactions involved, (s) = solid and (g) = gas.

One would assume that since 1) alumina and silicon carbide are totally immiscible in the solid state, and 2) since they ($\text{Al}_2\text{O}_3 + \text{SiC}$) do not form a compound, then the system $\text{Al}_2\text{O}_3 + \text{SiC}$ would be non-reactive. However, this may not be the case. The "native oxide" coating on the SiC is SiO_2 . This will react with Al_2O_3 to form mullite, thus:



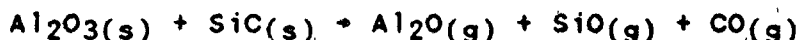
The SiC powder may also contain carbon (or a carbon-producing substance). A reaction is possible between the carbon, silicon carbide, and alumina to form the stable compound: aluminum silicon carbide, i.e.: Al_4SiC_4 or $\text{Al}_4\text{C}_3 \cdot \text{SiC}$, thusly:



The carbon monoxide (CO) that forms may lead to microporosity or, because of the internal gas pressure, may make densification more difficult. The alumina and silicon carbide may also react to form aluminum oxycarbides [Al_2OC or $(\text{Al}_2\text{O}_3 \cdot \text{Al}_4\text{C}_3)$ or $\text{Al}_2\text{O}_4\text{C}$ or $(4 \text{ Al}_2\text{O}_3 \cdot \text{Al}_4\text{C}_3)$] and high temperature mullite [Al_4SiO_8 or $(2 \text{ Al}_2\text{O}_3 \cdot \text{SiO}_2)$] thusly:



Unfortunately, the alumina and silicon carbide can also react to form all vapor species, thus consuming each other, thusly, e.g.:



It is not known at this time at what temperatures these reactions become significant, and what effects they may have on stability, densification, and the limits on the production of thick ceramic blocks; but suffice it to say that these reactions will be operable in the currently popular Al_2O_3 - silicon carbide whisker composites as well as in the Al_2O_3 - silicon carbide particulate composites investigated in this study.

In the formulating of many composite systems, the internal stresses caused by the difference in thermal expansion (or contraction) between the matrix and dispersed phase is not taken into consideration. Also, the thermal expansion (or contraction) anisotropy of the matrix is oftentimes forgotten or neglected. In some systems like silicon carbide whisker-reinforced, fully dense, fine-grain silicon nitride, the effect of the differential expansion may not be a problem and, in fact, may aid in strengthening the system or increasing its toughness because the reinforcing phase contracts more than the matrix in cooling.

and either puts the matrix in compression (if bonded to it) or shrinks away from the matrix (if not bonded to it), leaving microgaps which may make crack propagation more difficult.

In the case of Al_2O_3 -SiC, however, the situation is much different. Here the coefficient of thermal contraction for Al_2O_3 is approximately twice that of SiC from 2000K down to room temperature ($\alpha \text{ Al}_2\text{O}_3 \approx 10 \text{ ppm/K}$ and $\alpha \text{ SiC} \approx 5 \text{ ppm/K}$). Depending on the microstructure, this phenomenon can cause the generation of internal tensile stresses within the Al_2O_3 -SiC ceramic. Figure 10 is a diagrammatical representation of this situation. If the SiC grain is locked within the Al_2O_3 grain, it will put it in tension, but if the size ratio of Al_2O_3 :SiC is correct, it will cause the grain to be under tension; however it will not form a microcrack. Otherwise, a microcrack will form (pre-existing crack). However, when an external tensile load is applied to the already tensile loaded Al_2O_3 grain, the Al_2O_3 grain will fracture transgranularly (See Figure 11). If the SiC grains are all located at the grain boundaries, fracture will most likely take place intergranularly due to stress fields trying to separate the Al_2O_3 grain boundaries. As the figure shows, other types of microstructures will cause a combination of trans- and inter-granular fracture.

The reasons as to the cause of the different locations of the dispersed silicon carbide phase within the alumina matrix must be discussed at this point. If a mechanically-mixed system such as this were composed only of 100% chemically pure Al_2O_3 and SiC, the SiC would most likely end up at the grain boundaries and at the "triple points". This would occur because the SiC is neither soluble in nor wetted by the alumina. This situation then would cause all of the SiC grains to pin the grain boundaries of the Al_2O_3 and prevent them from growing. It would also make densification (even when pressure assisted) almost impossible. But, since the SiC particles most likely have a film of SiO_2 ("native oxide") on their surface, the wettability by Al_2O_3 is greatly enhanced. This however, would not be enough to cause the formation of a liquid grain boundary phase (most likely because of the formation of high temperature mullite) and the grains would still largely be "pinned" as in Figure 12(a). However, with the formation of a liquid phase grain boundary phase derived from the natural impurities in the alumina, viz., SiO_2 , Na_2O , Fe_2O_3 , CaO , MgO , and TiO_2 plus the "pick-up" from the grinding media and the impurities associated with the SiC, wetting and material transport will occur. This is shown diagrammatically in Figure 12(b), where the alumina grain boundary moves up to a silicon carbide grain and is temporarily "pinned" until the liquid

phase starts to wet the grain and allows alumina, dissolved in this "glassy" silicate phase, to move around the SiC grain, causing the alumina to grow around and encapsulate the SiC. Thus, grain growth and densification can proceed by mass transport around the SiC until it is impeded by other SiC grains.

In the case of the "pure", "single-phase" aluminas, the coarse-grained aluminas will have a significantly lower strength than the fine-grained aluminas, as shown in Figure 13, due to the large effect of the thermal contraction anisotropy (i.e., between the a and c axes) of each single crystal (i.e., each grain of the large grained alumina crystals work against each other in the polycrystalline mass). Here we can see that by increasing the average grain size by a factor of 4 (i.e., 5 to 20 μm), the strength (MOR_{max}) dropped by a factor of 2 (i.e., 60 to 30 kpsi).

Examining Figure 14, one can see that the overriding factor in the maximum strength achievable with the system $\text{Al}_2\text{O}_3\text{-SiC}$ is the grain size. When the dispersed silicon carbide grains pin the alumina grains and prevent grain growth, high strengths can easily be obtained. In this study, when the average alumina grain size was kept below 1 μm , maximum strengths approaching 100 kpsi could easily be obtained. As an example of the phenomena, pressure assisted sintering or densification (PAD) of "pure" Alcoa A-16 SG alumina at 1825°C yielded a ceramic with an approximately 20 μm average grain size and a maximum strength of only 33 kpsi, while the addition of 30 % fine SiC to this same matrix caused the average grain size to drop dramatically to 0.64 μm and the maximum strength to jump to 111 kpsi.

The concept of maximum strength was introduced into the analyses of the mechanical properties of this system. Since the system, $\text{Al}_2\text{O}_3\text{-SiC}$, is loaded with internal tensile stresses, microcracks may form during cooling, handling, and machining of the $\text{Al}_2\text{O}_3\text{-SiC}$ (particulate) composites. It is assumed that the maximum MOR (modulus of rupture) measured represents the potential of the mechanical properties of the system free from prematurely developed cracks. To test this hypothesis, strength data from a duplicate run was plotted as a histogram of strength distribution, singly and combined. The result is shown in Figure 15. It shows a well-defined peak with a long tail extending towards a strength of zero kpsi, indicative of many, extremely weak, cracked specimens. If the distribution were truncated through proof testing or the population otherwise refined, then the histogram might look like the non-crosshatched area in Figure 16(b). Figure 16(a) shows a uniformly flawed (microcracked) ceramic that has a very uniform tensile stress field throughout and where maximum strength is very

close to its mean strength. This situation actually occurred when ALCOA A-16 SG alumina was composited with 10 V/o of coarse-grained SiC (See Figure 17). This material was densified with pressure assistance at 1600°C. The combination of the internal stress produced by the coarse SiC particle acting on the Al₂O₃ grains, plus the internal stress of the Al₂O₃ grains acting on themselves gave rise to a uniformly microcracked (i.e., totally "flawed") microstructure resulting in an extremely high Weibull modulus (m) (approaching 50), with a moderate but acceptable strength of 60 kpsi. (See Figure 17.) This ceramic would have an extremely predictable load bearing characteristic making it useful as a structural ceramic as well as a potential lightweight ceramic armor system.

The question of the use of these materials as effective armor must be explored. Certainly the goal of producing a strong, lightweight, hard, ceramic material from low cost raw materials (e.g., commercial ceramic-grade alumina and abrasive-grit-grade silicon carbide) was met. The question is: What will be the performance of these materials as armor? If one subscribes to the hypothesis that a ceramic with transgranular fracture is the best performing as armor₂, then there are materials in this system that will, potentially, perform extremely well. If one subscribes to the hypothesis that intergranular fracture is best₃, then these materials exist in this group and, lastly, if mixed mode fracture is shown to be the best₂, then this study also produced this type of material.

However, if one prescribes to the hypothesis that the retained strength after fracture in a confined system is best, then this study produced one of the best candidates to be considered as a model for this hypothesis. If one examines the residual strength of a faulted system (σ_{sf}) after large strains as in Figure 18, then a ceramic which granulates into a fine powder upon fracture might be the best candidate for an armor system₄. If the Weibull modulus is large, as in a highly anisotropic, highly internally stressed light-weight ceramic armor material such as TiB₂², it might perform similarly to TiB₂. With the Al₂O₃ - 10 V/o SiC (particulate) ceramic developed in this study, this material, with its strength of 60 kpsi and Weibull modulus

2 TiB₂ hot pressed ceramic is normally a coarse-grained, internally stressed ceramic because of a large difference in thermal expansion between the a and c axes of its hexagonal grains. Also, each grain is further highly strained because of the precipitation of TiC within each grain. Carbon (available during the reaction $2 \text{TiO}_2(s) + 3 \text{C}(s) + \text{B}_4\text{C}(s) \rightarrow 2 \text{TiB}_2(s) + 4 \text{CO}(g)$) is soluble in TiB₂ but the metastable solid solution breaks down on reheating, forming a fine dispersion of TiC within the already highly-stressed TiB₂ crystallites.

of around 50 is so completely flawed, that is, totally networked with microcracks it might break up very easily into tiny fragments upon ballistic impact and form a compacted powder that, when completely constrained, is so dense that it might prevent the further penetration of a projectile.

6.0 CONCLUSIONS:

1. The strength of fully dense alumina (or its composites with SiC particulates) is controlled, largely, by the Al_2O_3 grain size.

2. The addition of silicon carbide (SiC) particulates to alumina (Al_2O_3) significantly reduces the grain size of the alumina.

3. The addition of 10 % of a low cost SiC to a low cost alumina results in a ceramic with a Weibull modulus approaching 50. This material is expected to have good ballistic resistance since its uniformly flawed structure will yield a granulated debris with high residual strength when constrained. (This type of ceramic will also find use in structural applications because of the superior predictability of its strength characteristics.)

4. Cercom's proprietary alumina ceramic compositions containing 10 % of a low-cost SiC performed as well as or better than MTL's base-line sintered alpha silicon carbide (Carborundum's Hexaloy).

7.0 REFERENCES

1. Rice, R. W., "Toughening in Ceramic Particulate and Whisker Composites", Ceram. Eng. Sci. Proc. 11 [7 - 8] pp. 667 - 694 (1990).
2. Shockey, D.A., Marehand, A. H., Skaggs, S. R., Cort, G. E., Burkett, M. W., and Parker, "Failure Phenomenology of Confined Ceramic Targets and Impacting Rods", Int. J. Impact Engrg. 9 [3] pp. 263 - 275 (1990)
3. Tracy, C., Slavin, M., and Viechnicki, D., "Ceramic Fracture During Ballistic Impact", U. S. Army MTL, Presented at "Fractography of Glasses and Ceramics Conference", Alfred University, 3 - 6 August 1986.
4. Johnson, G. R., Holmquist, T. J., Lankford, V., Anderson, C. E., and Walker, "A Computational Constitution Model and Test Data for Ceramics Subjected to Large Strains, High Strain Rates, and High Pressures", Contract DE-AC04-87AL-42550, Final Technical Report for Optional Task I, August 1990.

Table 1. Raw Materials

Material	Mfg.	Designation	Volume Pricing \$/Pound	Particle Size*	Surface Area* (M ² /g)
Al ₂ O ₃	Ceralox	HPA	\$ 4.80	0.5	10
Al ₂ O ₃	Alcoa Aluminum	A-16 SG	\$ 1.75	0.45	8.7
SiC	H. C. Starck	Beta 10	\$10.50	0.4	14-17
SiC	Lonza	UF-15	\$ 9.00	0.8	15
SiC	Lonza	F-1000	\$ 3.60	4.8	N/A

* As Provided by Suppliers

Table 2. Residual Penetrations and Penetration Reductions for Impacts at 1500 m/s on Cercom Incorporated Samples

Test No.	Sample Ident.	Areal Density (g/cm ²)	Proj L/D	Residual Penetration (mm)	Penetration Reduction (mm)	Scaled Penetration Reduction (mm/g/cm ²)
SiC-B						
76	4-367-1A	8.16	10	35.2	34.9	4.28
77	4-367-1B	8.19	10	22.5	48.7	5.95
78	4-367-1C	8.19	15	52.6	37.9	4.63
79	4-367-2A	12.29	10	13.5	58.7	4.78
80	4-367-2B	12.24	10	17.6	55.3	4.52
81	4-367-2C	12.23	15	39.4	49.3	4.03
85	4-388-1A	16.37	10	0.0	71.9	4.39
86	4-388-2A	16.30	15	25.1	62.3	3.82
87	4-388-3A	16.32	15	27.4	60.0	3.60
EBON-A						
82	4-363-1A	10.08	10	42.9	29.6	2.94
83	4-363-1B	10.01	10	37.7	33.8	3.38
84	4-363-1C	10.11	15	48.9	37.9	3.75
88	4-363-2A	15.00	15	23.4	65.4	4.36
89	4-363-2B	15.13	15	45.0	42.6	2.82
90	4-363-2C	15.15	15	21.7	64.1	4.23

Table 3. Comparison of Scaled Penetration Reductions of Baseline AD90 and Cercom Incorporated Ceramics

Material	Proj. L/D	Average Areal Density (g/cm ²)	Average Scaled Penetration Reduction (mm/g/cm ²)	AD90 Scaled Reduction For Areal Density (mm/g/cm ²)	Material AD90
SiC-B	10	8.18	5.11	2.68	1.907
SiC-B	15	8.19	4.63	3.07	1.507
SiC-B	10	12.26	4.65	2.44	1.906
SiC-B	15	12.23	4.03	2.67	1.511
SiC-B	10	16.37	4.39	2.19	2.004
SiC-B	15	16.31	3.75	2.26	1.657
EBON-A	10	10.04	3.16	2.57	1.230
EBON-A	15	10.11	3.75	2.88	1.302
EBON-A (high)	15	15.08	4.30	2.38	1.807
EBON-A (low)	15	15.13	2.82	2.38	1.185

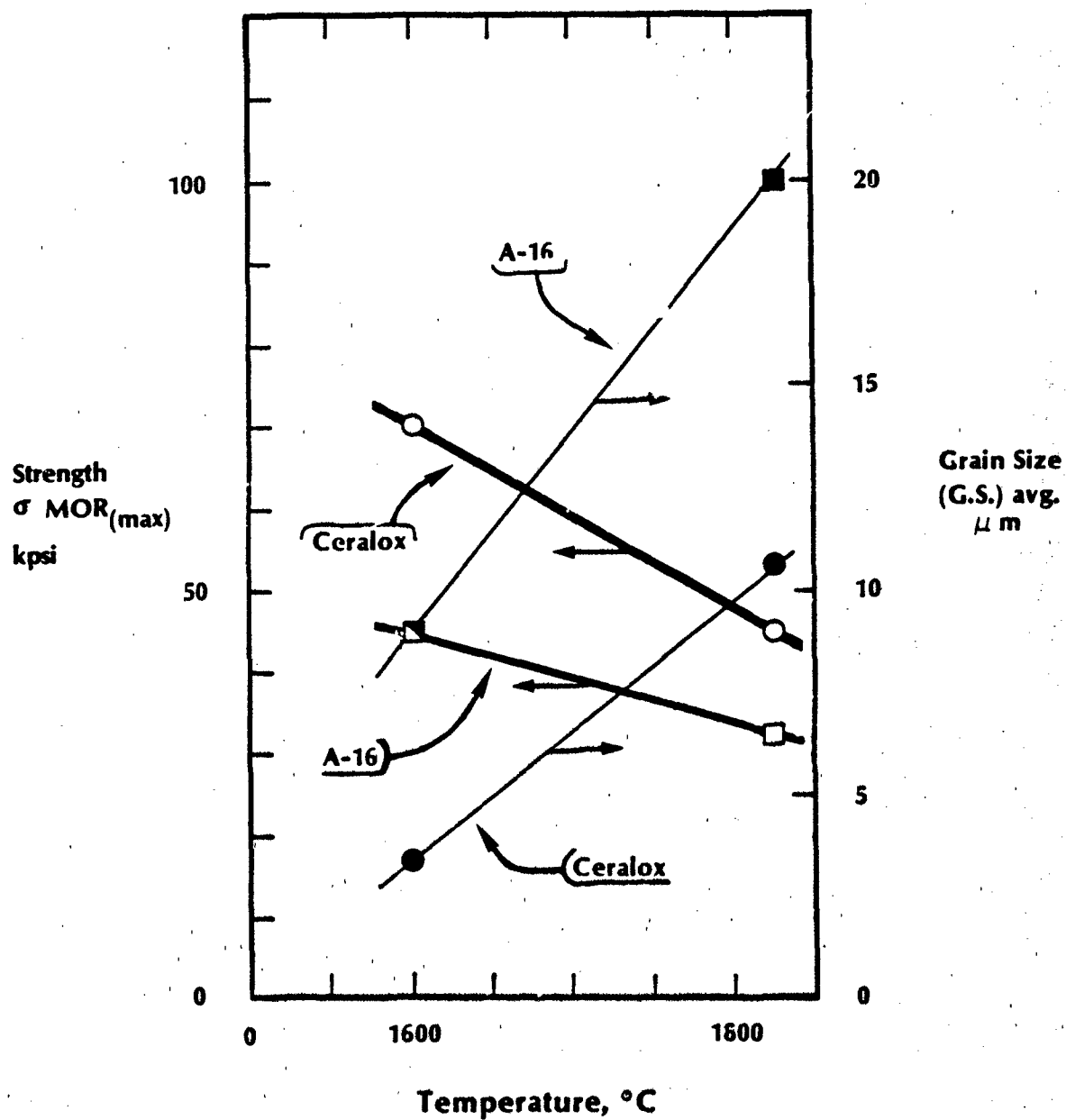


Fig. 1 — Effect of pressure assisted densification (PAD) on the strength and grain size of "pure" alumina.

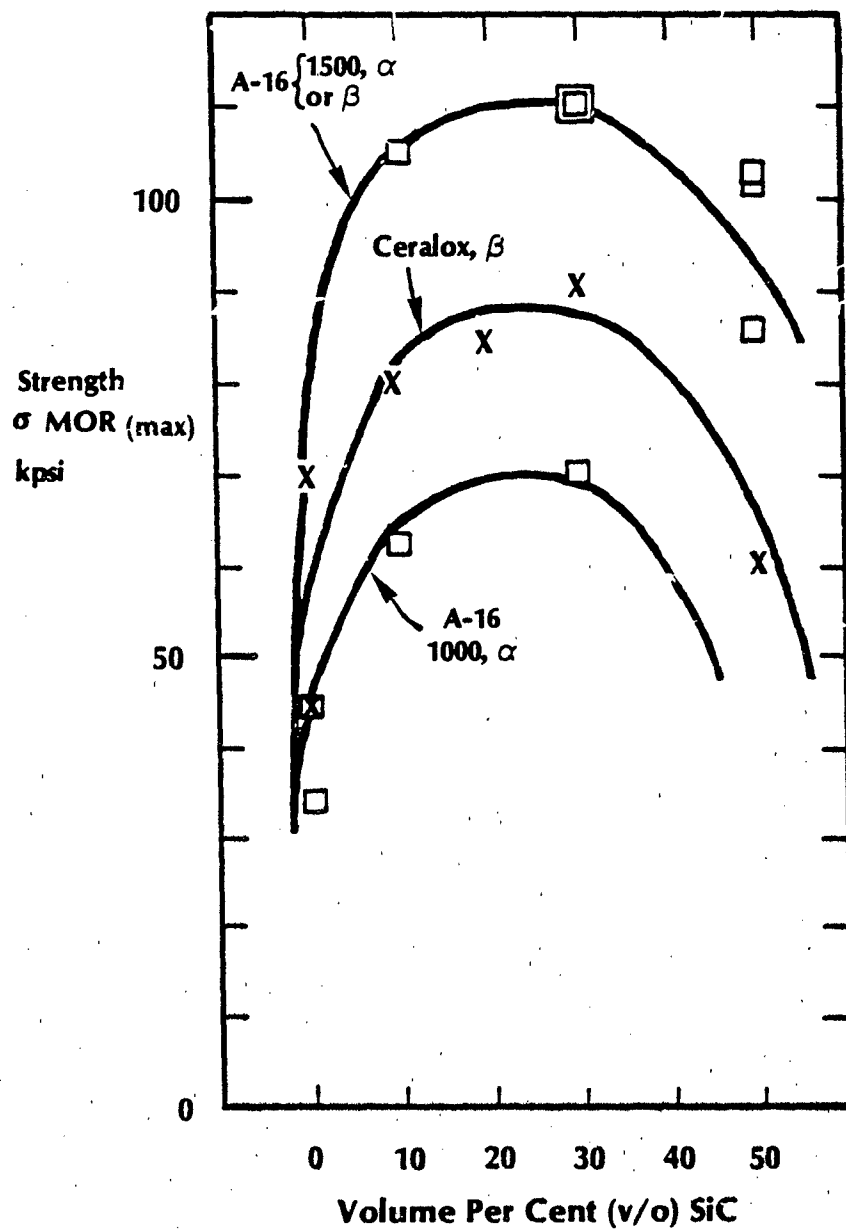


Fig. 2 — Effect of v/o SiC on the strength of hot pressed alumina

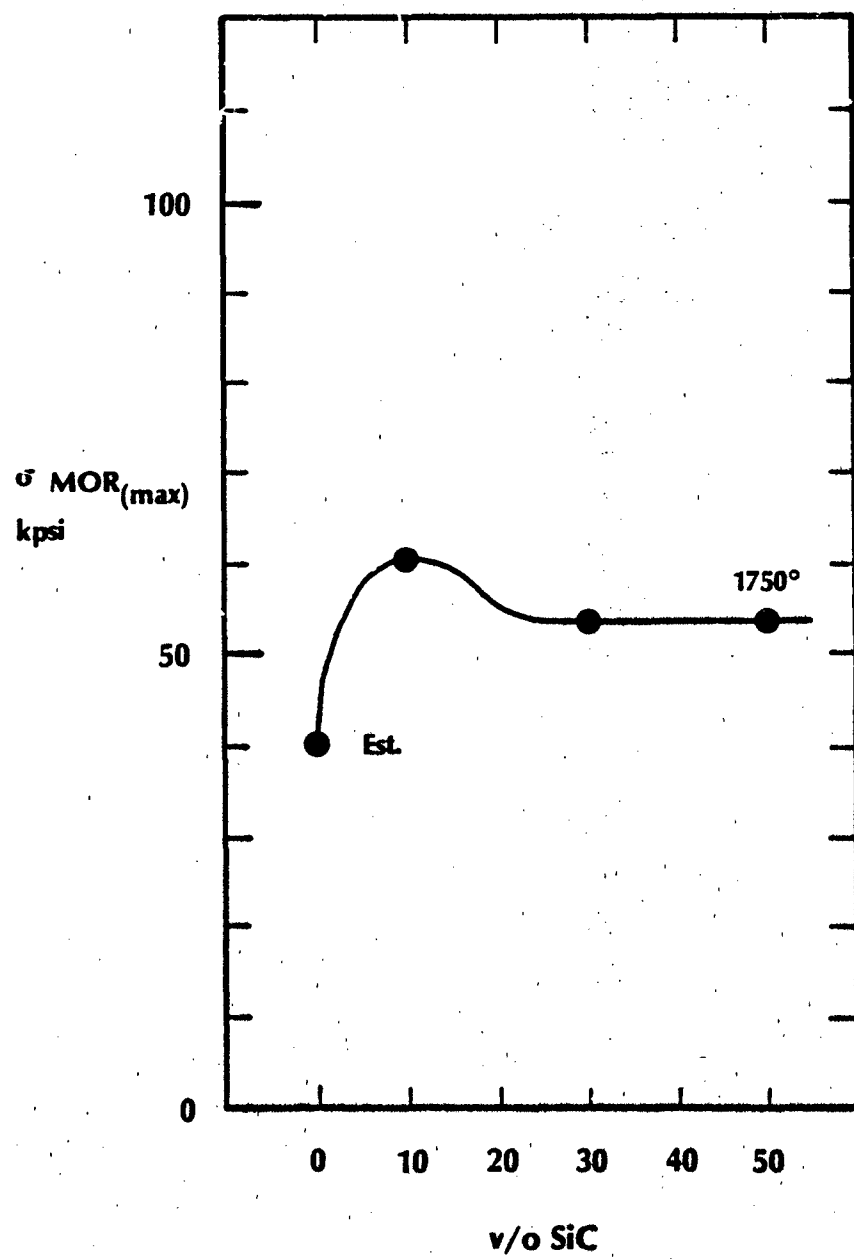


Fig. 3 — Effect of Volume % SiC on the strength of composites Pressured Assisted Densified (PAD) at 1750°.

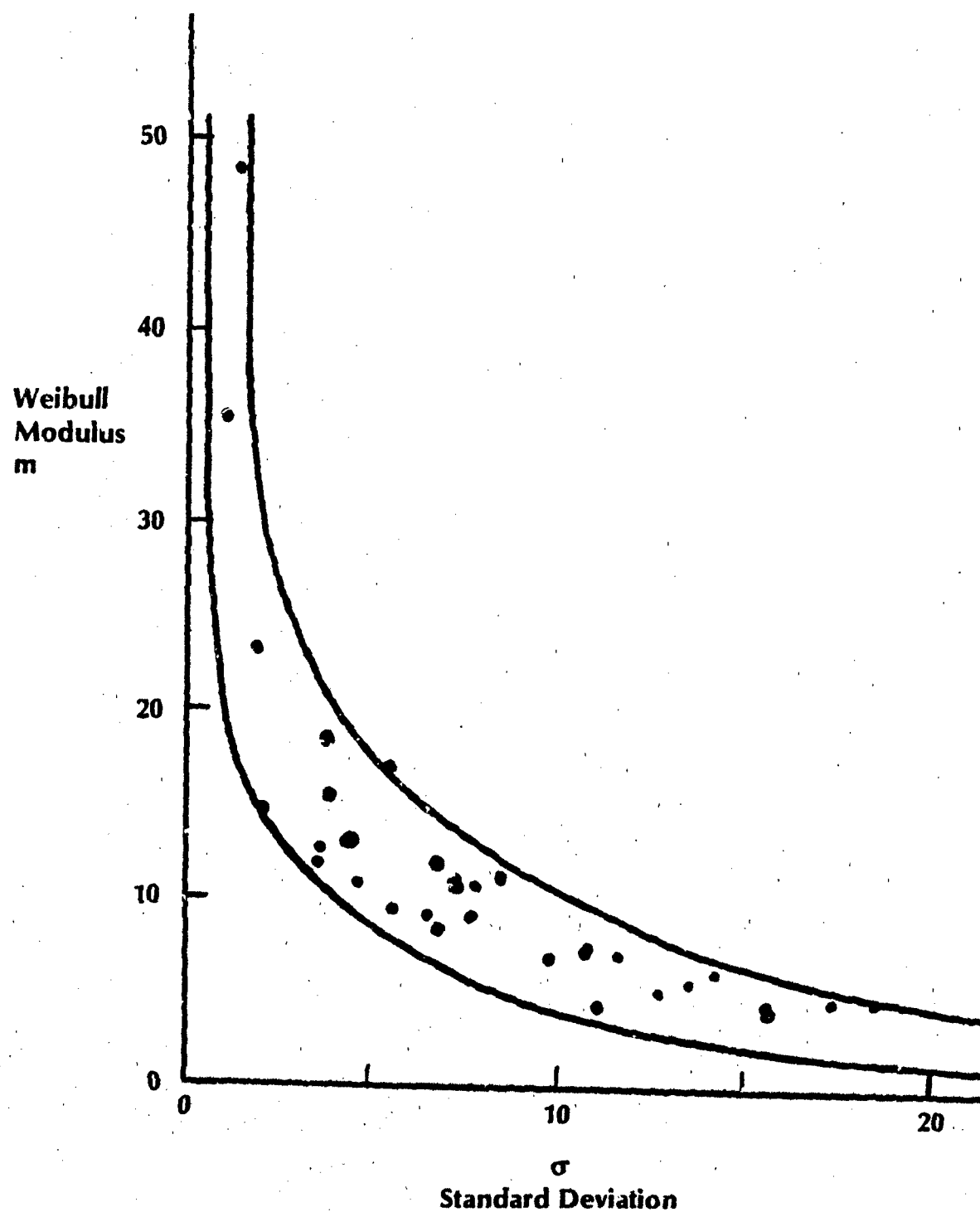


Fig. 4 -- Relationship between Weibull modulus (m) and standard deviation (σ) of strength measurement (MOR-4 pt).

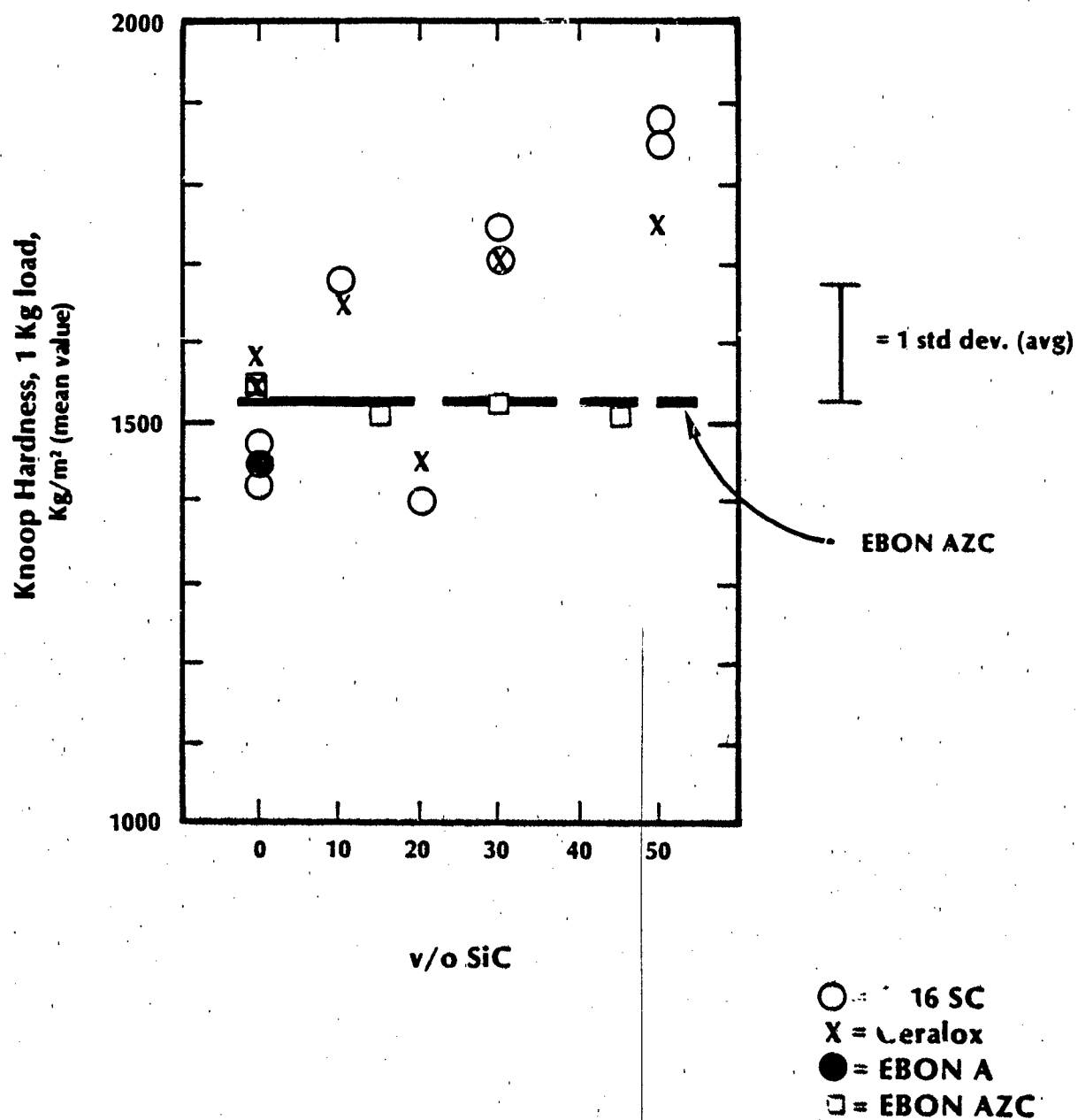


Fig. 5 — Effect of v/o SiC on the hardness of Al₂O₃ - SiC composites.

UNCLASSIFIED

Fig. 6 — Aluminum oxide comparisons.

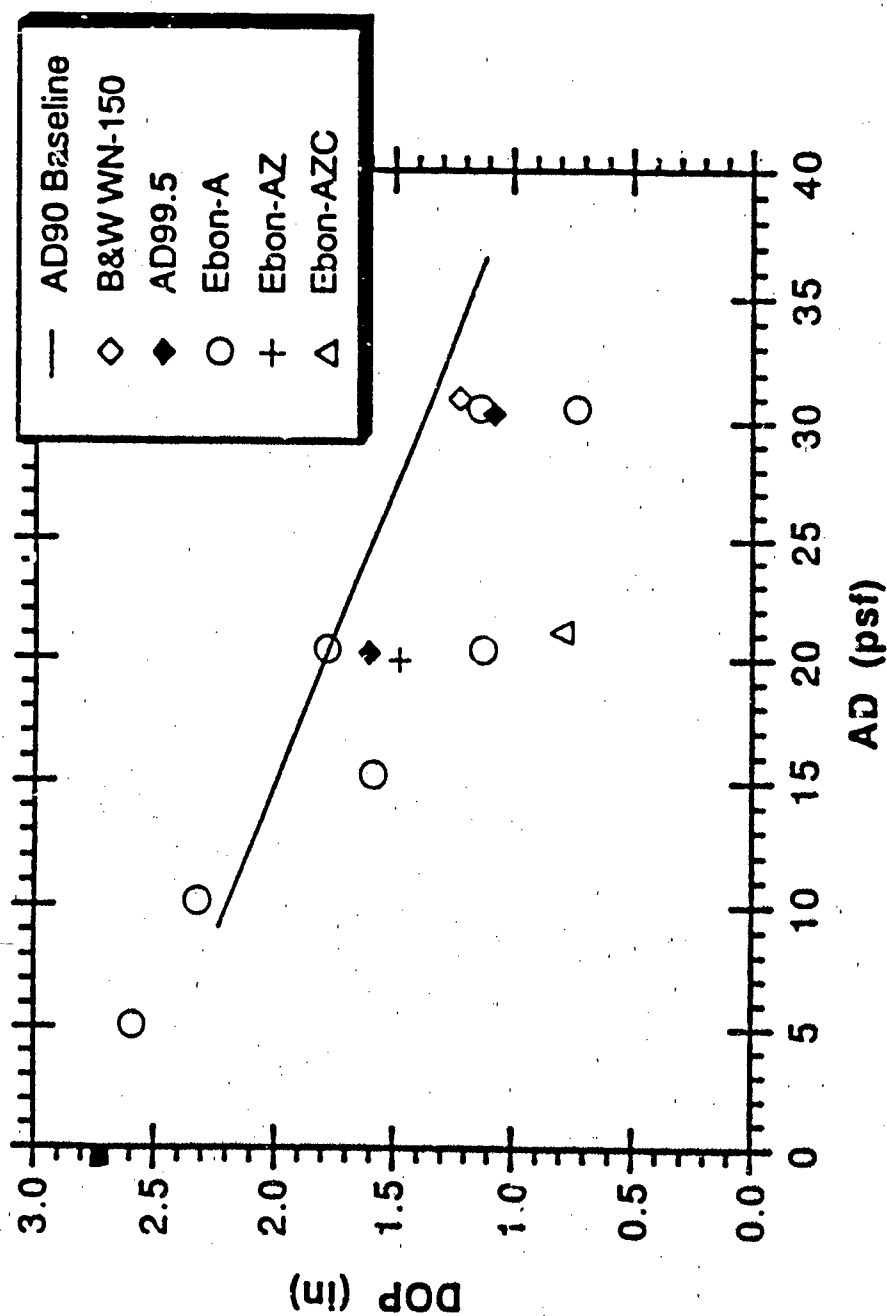
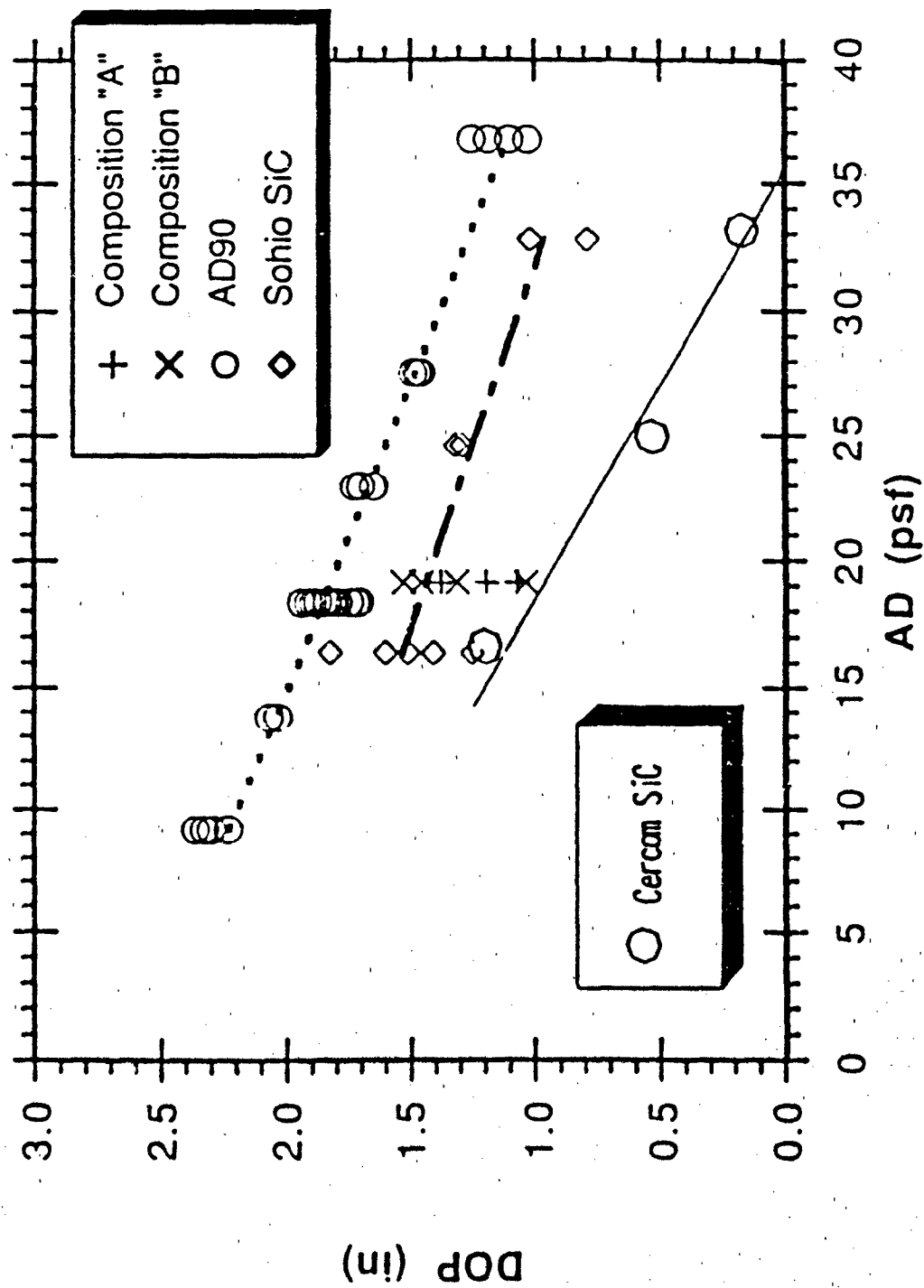
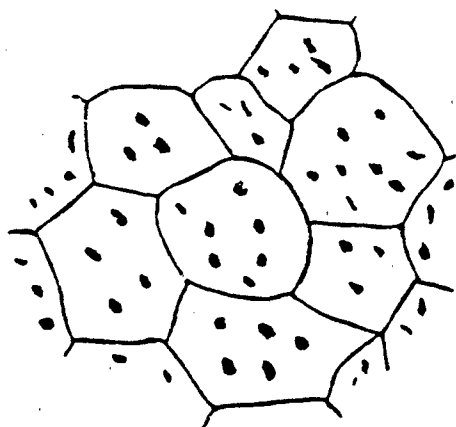


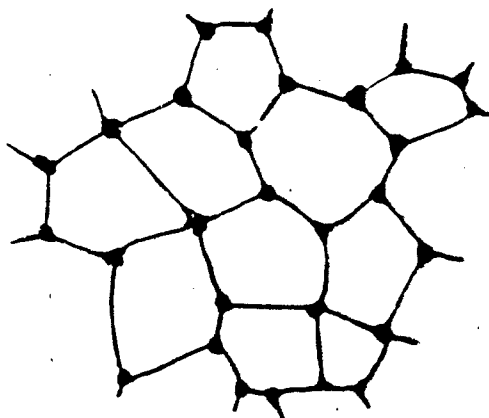
Fig 7 — Al_2O_3 - SiC composites performance.



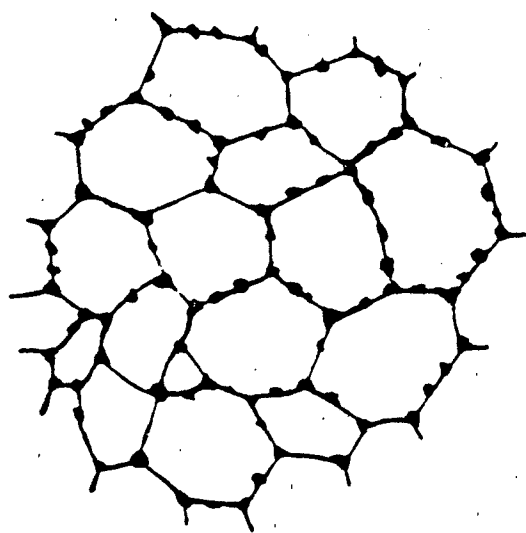
2/11/91
Courtesy of
US Army MTL



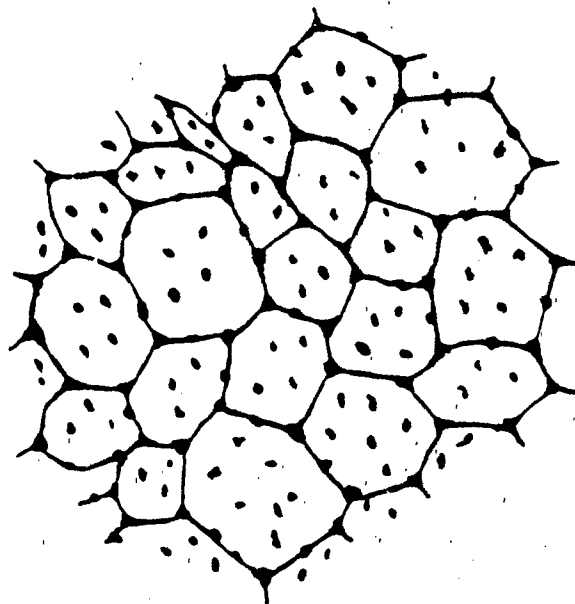
**All SiC grains
within Al_2O_3 grains**



**All SiC grains located
at the triple-points
of Al_2O_3 grains**



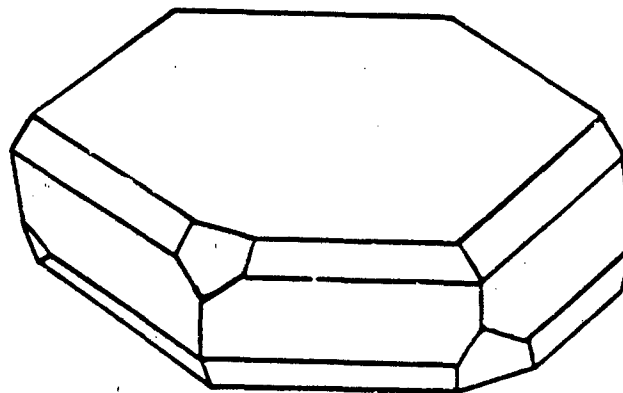
**All SiC grains located
along Al_2O_3 grain boundaries
including triple-points**



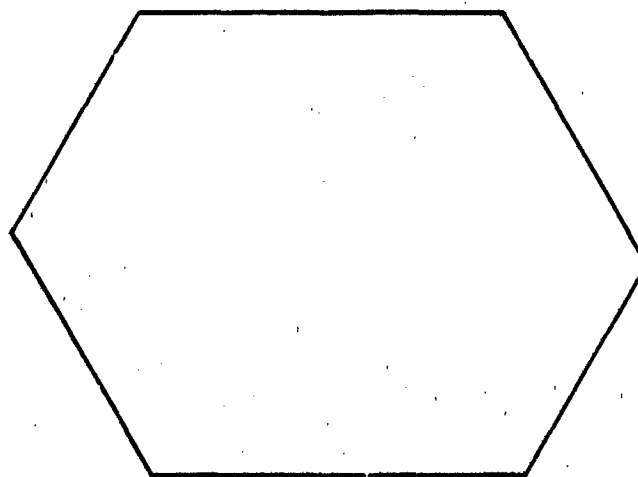
**SiC grains located
within the Al_2O_3 grains
and along the Al_2O_3 grain
boundaries as well as
at the triple-points.**

Fig. 8 — Idealized microstructures in the system Al_2O_3 - SiC

I 3-D



**II Cross-section
parallel to
basal plane**



**III Cross-section
at right angles
to the basal plane**

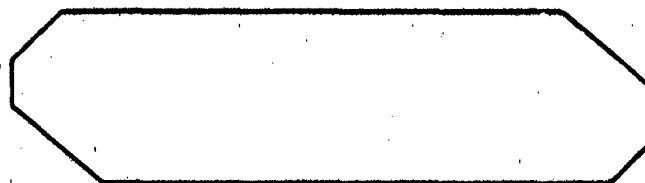
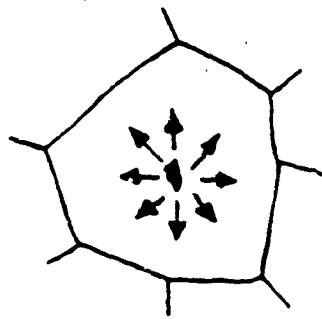
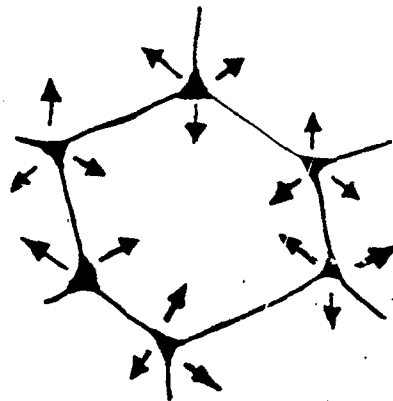


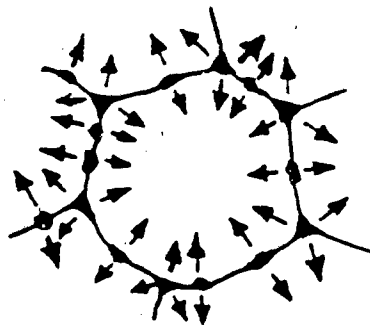
Fig. 9 — Morphology of alumina grain.



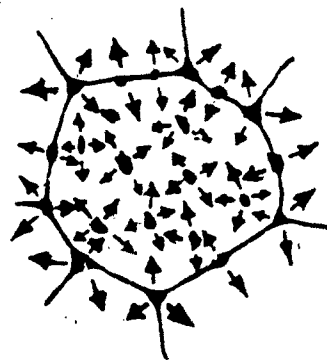
Transgranular Fracture



Intergranular Fracture with some transgranular fracture



Intergranular fracture



Mixed mode fracture, i.e. both intergranular and transgranular



	Material	Hi-temp coeff of expansion
	Al_2O_3	$\alpha \cong 10 \times 10^{-6}/^\circ\text{C}$
	SiC	$\alpha \cong 5 \times 10^{-6}/^\circ\text{C}$

Fig. 10 — Idealized microstructures and direction of residual stresses.

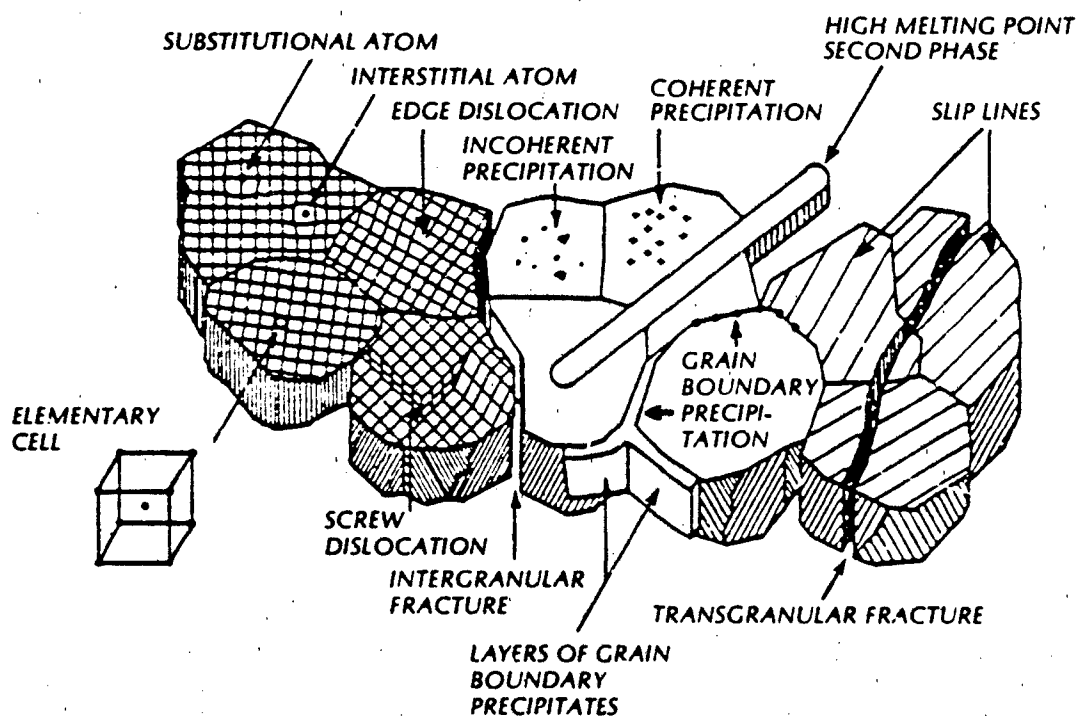


Fig. 11 — Schematic of microstructural features in materials.

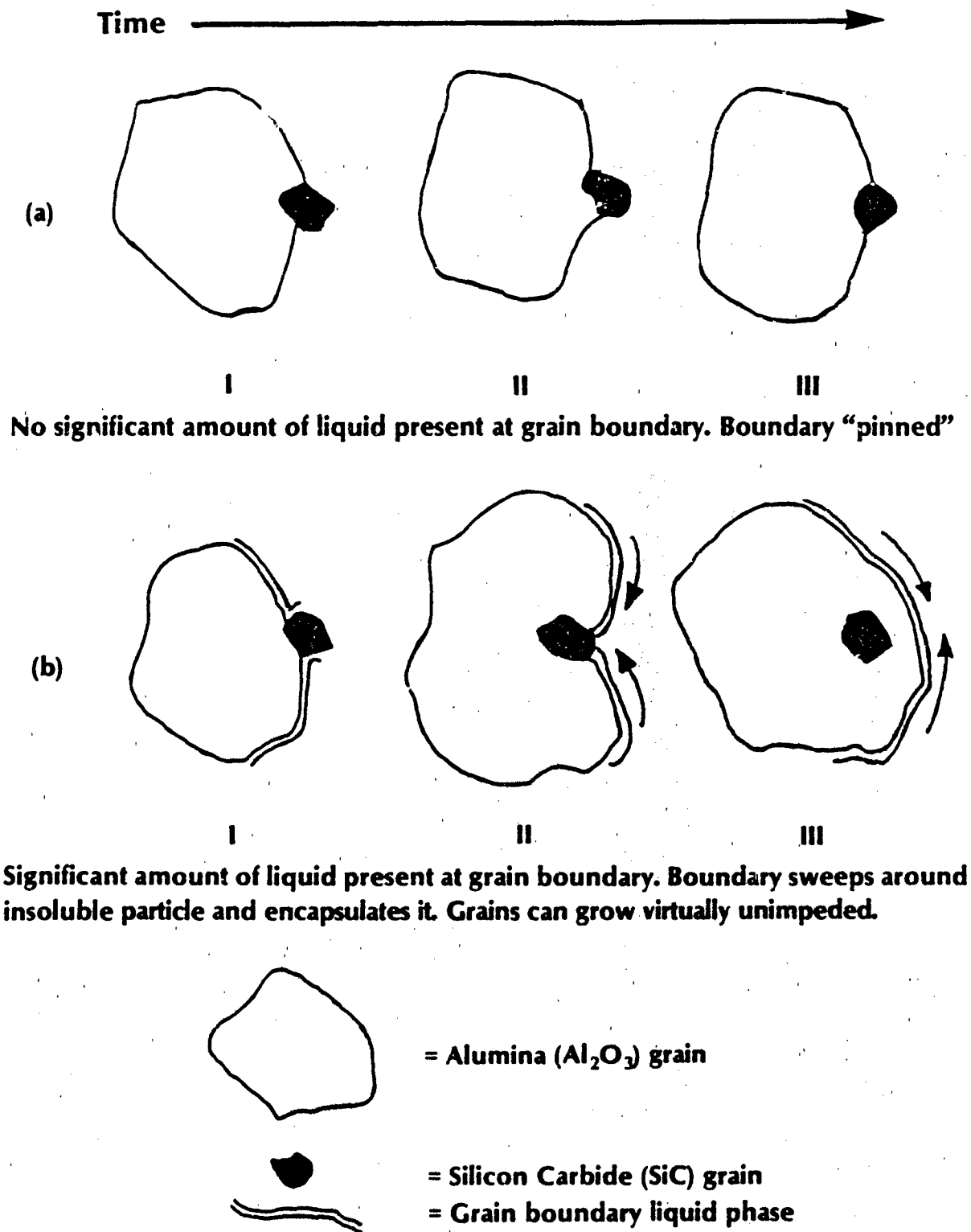


Fig. 12 — Development of Microstructures in Al_2O_3 - SiC composites.

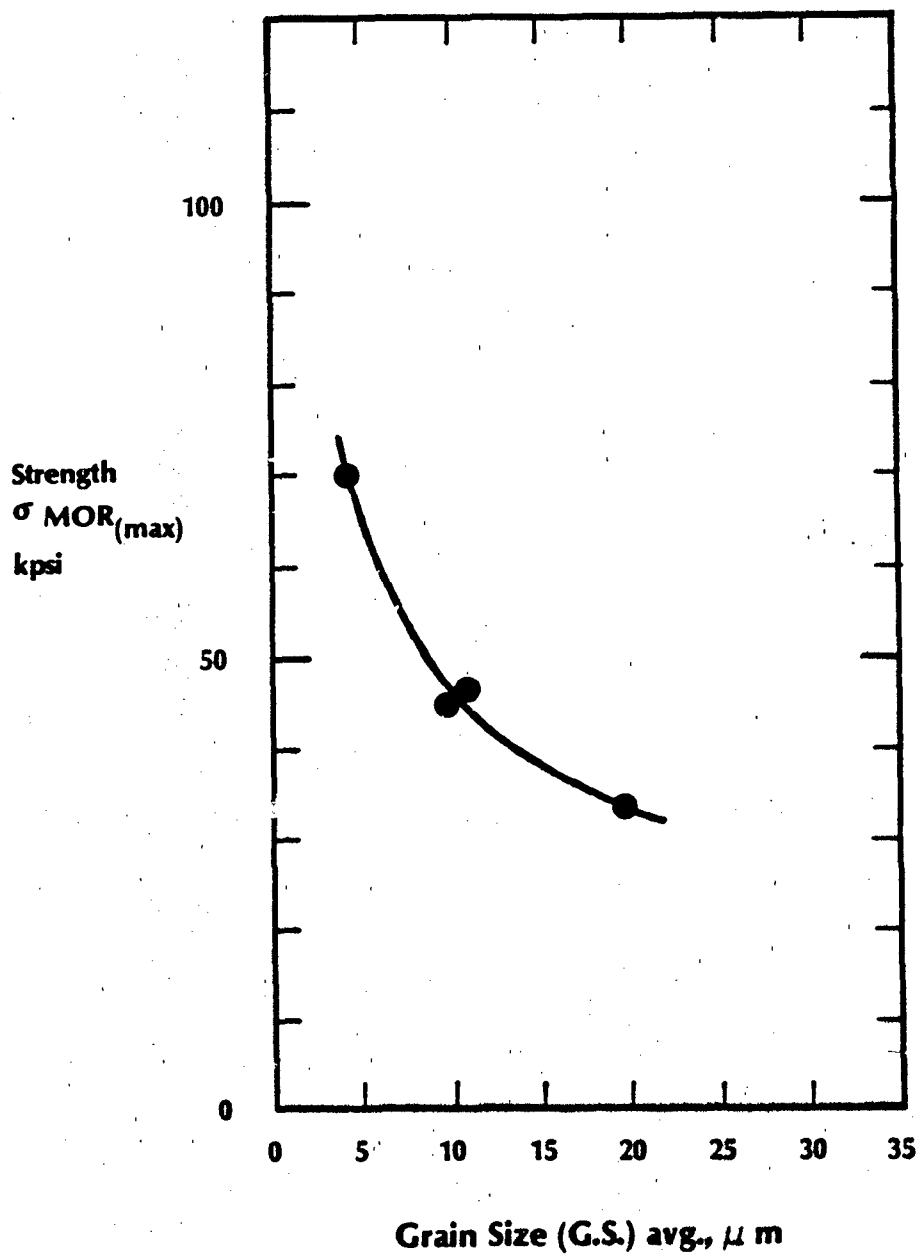


Fig. 13 — Effect of grain size on the strength of "pure" hot pressed alumina.

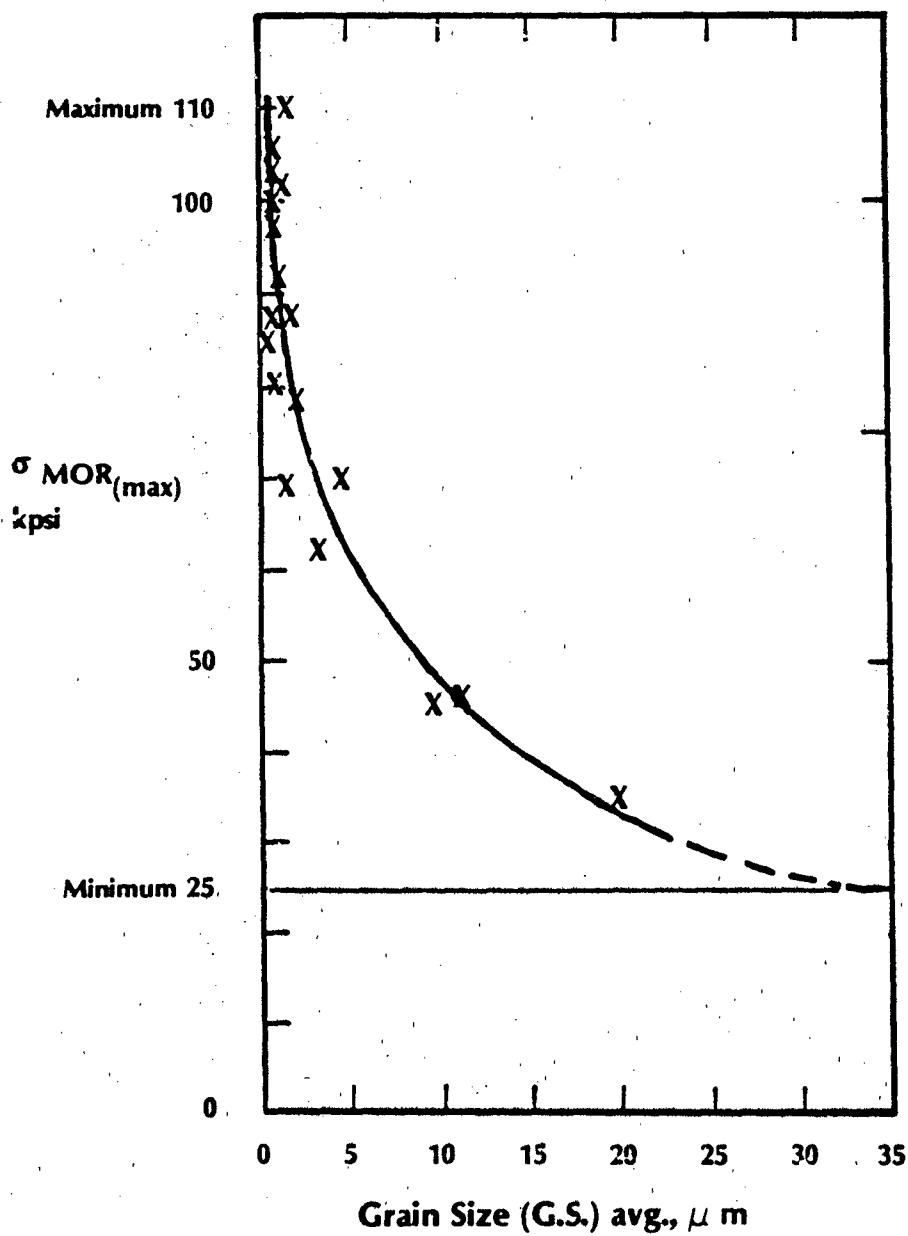
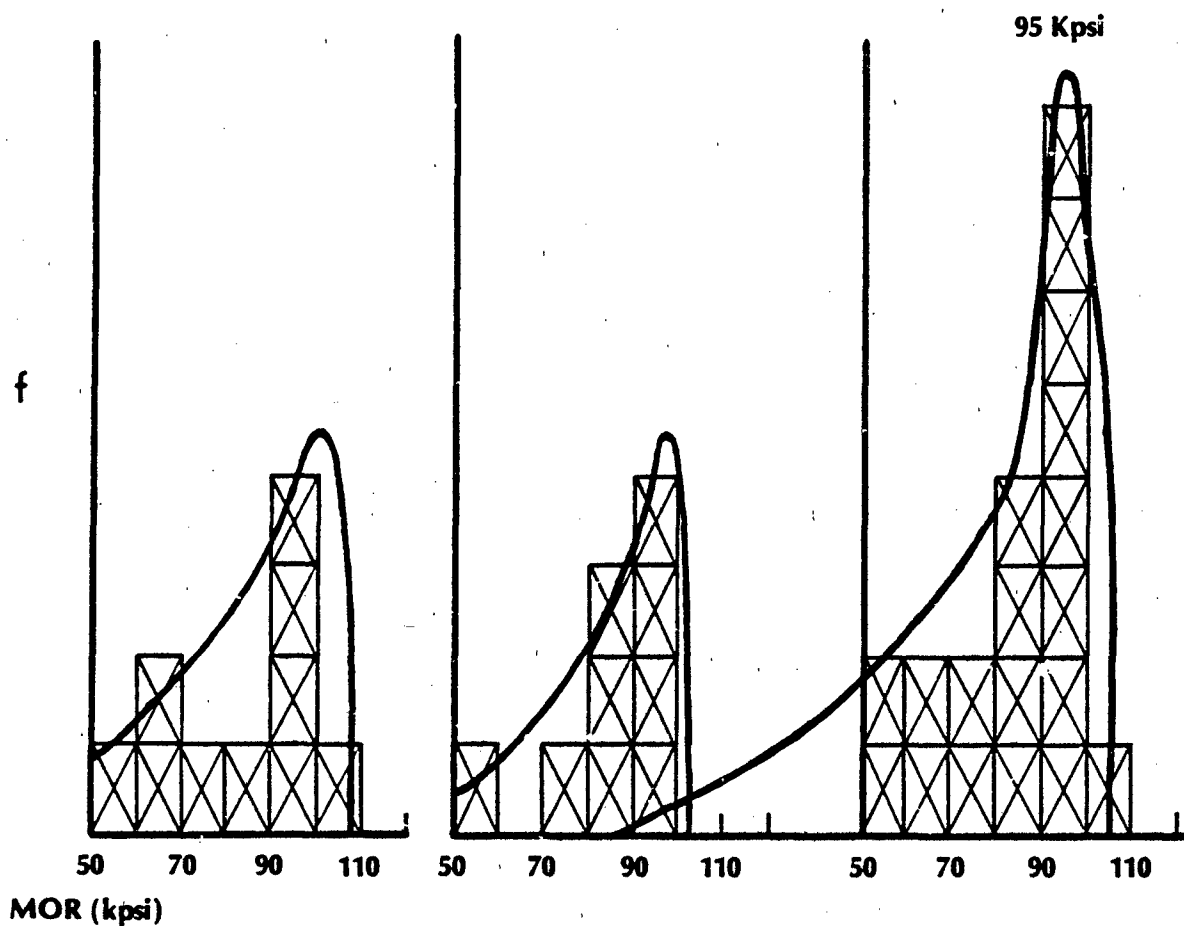


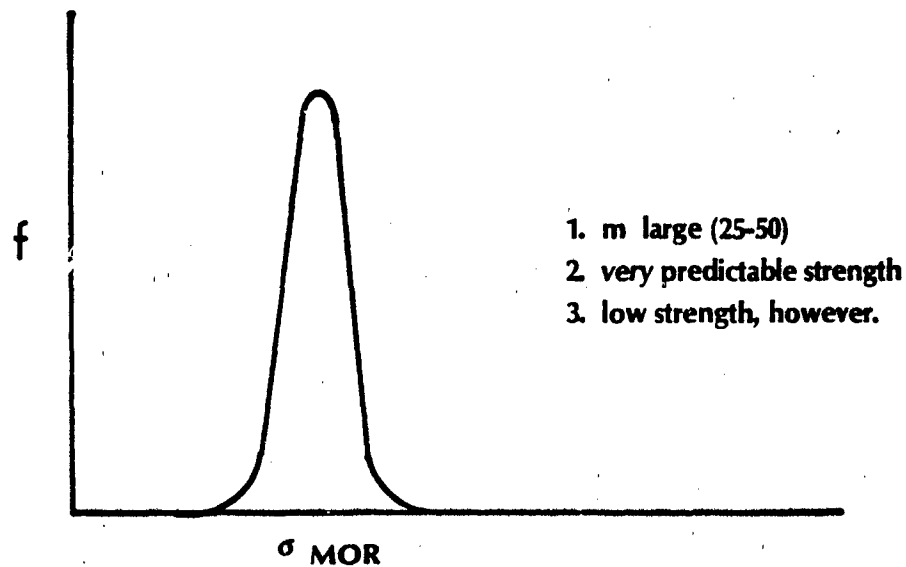
Fig. 14 — Effect of average grain size on the strength of alumina ceramics (with or without SiC).



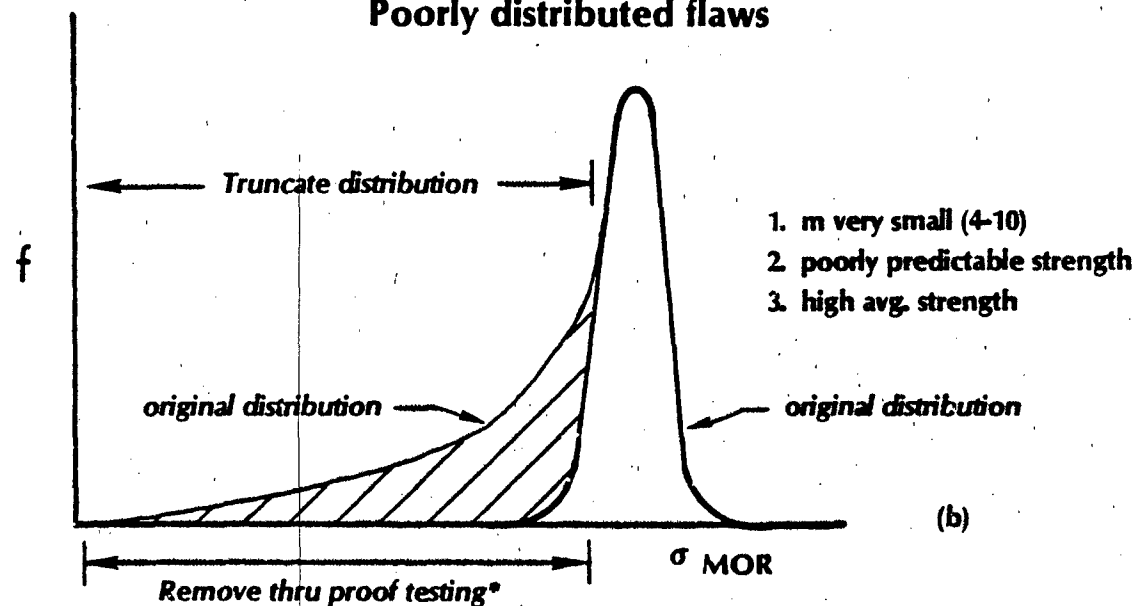
	<u>660-7B</u>	<u>660-7A</u>	<u>660-7</u>
No. of Samples	$n = 10$	9	19 (i.e. A + B)
Mean	$\bar{x} = 83.4$	83.3	83.4
One std. deviation	$\sigma = 17.3$	13.3	15.1
Coefficient of variation	$cv = 20.7\%$	16.0%	18.1%
Weibull Modulus	$m = 4.56$	5.85	~ 5.2

Fig. 15 — True histograms of strength distribution of two samples of 50 v/o Al_2O_3 - 50 v/o SiC (Alcoa A-16 SG — Lonza 15 UF) — singularly and then combined.

Unusual Ceramic Uniformly flawed



Typical "Advanced" Ceramic Poorly distributed flaws

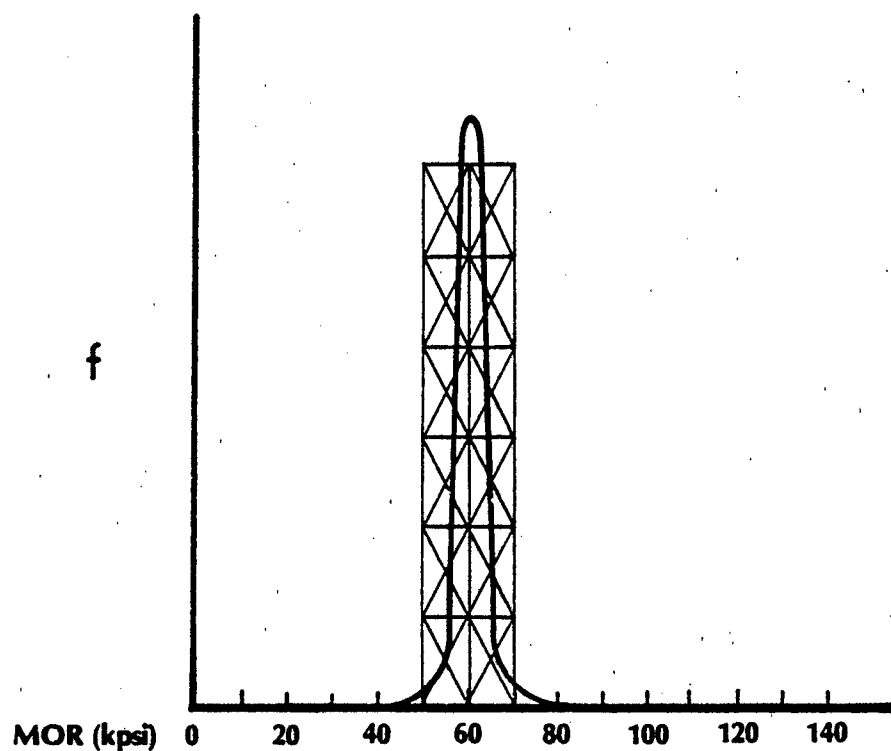


*then m larger. (Because of predictable strength.

Potentially good engine material.)

Fig. 16 — Schematic histograms of strength distribution.

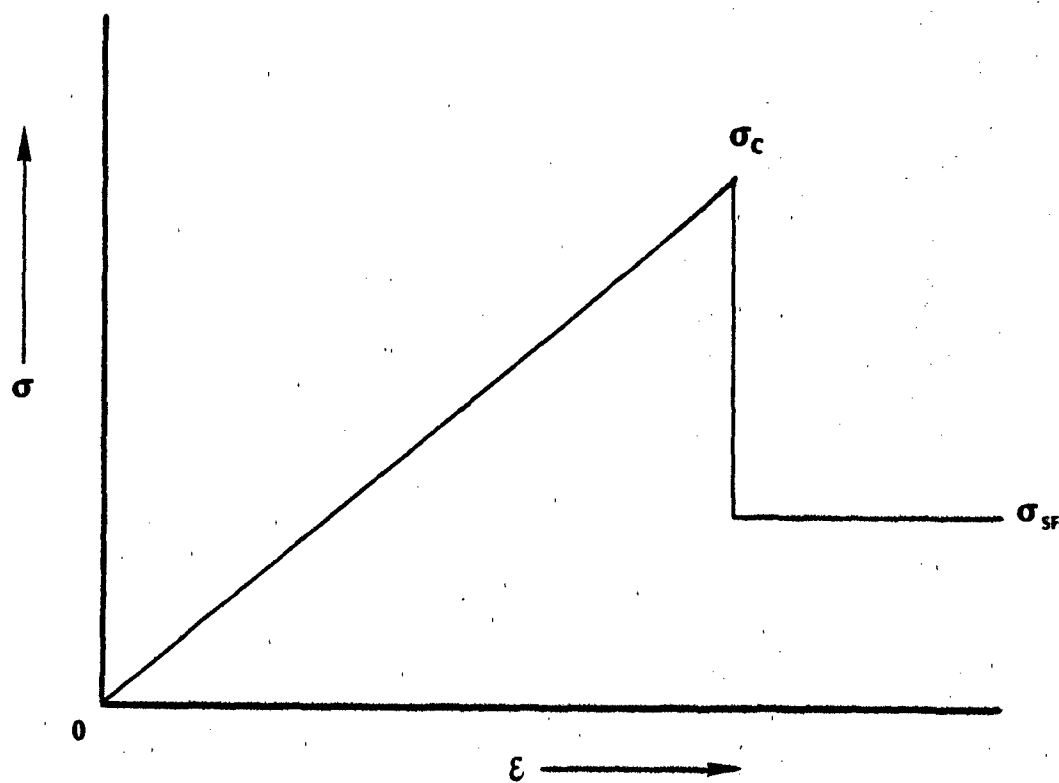
90 v/o Al_2O_3 — 10% SiC
(ALCOA A-16 SG - Lonza 1000 grit)



763-3

Mean \bar{x} = 60.1 kpsi
One std. deviation σ = 1.4 (6σ = 8.4 kpsi)
Range R = 57.9 - 62.2 kpsi
Weibull Modulus m = 48.4 ± 4.7

Fig. 17 — Al_2O_3 composite with unusually high Weibull modulus.



σ = strength
 σ_c = compressive strength
 σ_{sf} = residual strength of faulted system
 ϵ = strain

Fig. 18 — Retained strength after compressive failure of a constrained ceramic target.

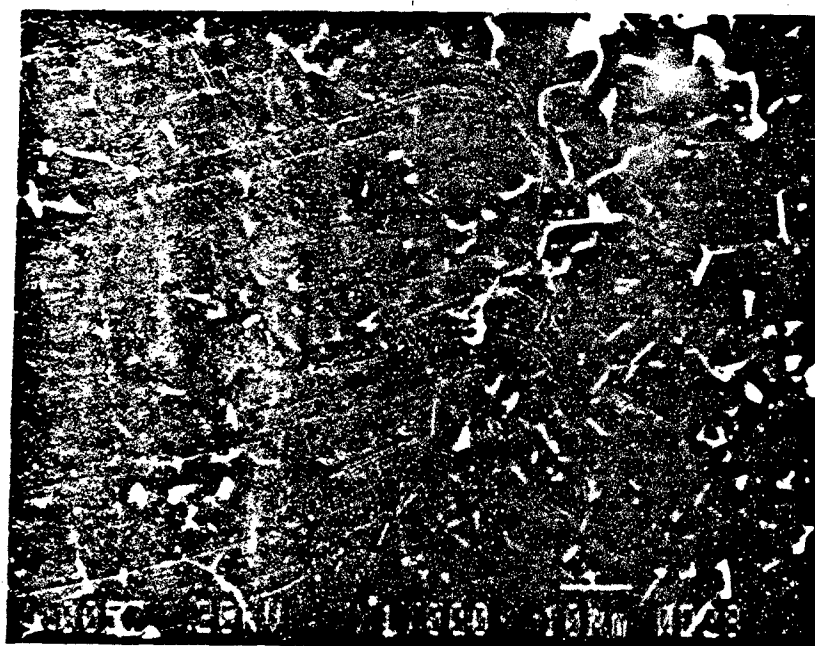
APPENDICES

RUN #	COMPOSITION, v/o		TEMP	DENSITY		% OF THEOR	GRAIN SIZE µm, avg.	K _{IC} MPa·m ^{1/2}	Knoop HARDNESS	HOB		KPSI avg.	KPSI max.	WEIBULL
	Al2O3	SiC		ACT	THEOR					MPa				
				g/cc										
7-1	100 Ceralox	0	1600 c	3.987	3.99	99.9	3.75	*	1556	62.03	427.7	70	18.34	
7-2	90 Ceralox	10 Beta	1600 c	3.893	3.91	99.6	.85	3.56	1653	70.08	483.2	80	9.4	
7-3	80 Ceralox	20 Beta	1600 c	3.779	3.83	98.67	.48	2.73	1556	74.26	512	85	5.4	
7-4	100 A-16	0	1600 c	3.979	3.99	99.7	9.09	*	1431	42.05	289	45	14.8	
7-5	90 A-16	UF-15	1600 c	3.905	3.91	99.9	.73	3.35	1677	94.4	650.9	106	11.7	
7-6	80 A-16	UF-15	1600 c	3.662	3.83	95.6	----	----	----	75.9	523.3	85.9	12.6	
0-3	100 A-16	0	1825 c	3.982	3.99	99.8	19.8	*	1477	32.3	222.4	33	35.6	
0-4	70 A-16	30 SiC Beta	1825 c	3.718	3.75	99.1	.97	3.01	1690	77.63	535.2	111	4.30	
0-5	50 A-16	50 SiC Beta	1825 c	3.571	3.60	99.2	.64	2.73	1831	75.75	522.27	85	10.8	
0-6	70 A-16	30 SiC UF-15	1825 c	3.723	3.75	99.3	.64	3.05	1759	92.2	635.8	111	6.32	
0-7A	50 A-16	50 SiC UF-15	1825 c	3.55	3.60	98.6	.86	2.73	----	83.3	574.6	100	5.85	
0-7B	50 A-16	50 SiC UF-15	1825 c	3.55	3.60	98.6	.75	2.80	1862	83.4	574.9	102	4.56	
4-1	100 Ceralox	0	1825 c	3.99	3.99	100	10.3	*	1568	43.2	298.1	45.5	23	
4-2	70 Ceralox	30 SiC Beta	1825 c	3.718	3.75	99.1	1.55	2.70	1704	80.3	553.9	98	11.5	
4-3	50 Ceralox	50 SiC Beta	1825 c	3.56	3.60	98.89	1.24	2.78	1760	55.4	382.0	60.2	13	
4-4	100 Ebon AZC	0		4.108	4.11	100	----	*	1550	48.5	334.4	53.9	11	
4-5	70 Ebon AZC	30 SiC Beta	1825 c	3.853	3.84	100	1.53	6.95	1516	45.5	313.7	50.1	13	
4-6	55 Ebon AZC	45 SiC Beta	1825 c	3.672	3.70	99.2	1.19	6.27	1488	53.2	366.8	60.2	16	
337-4	85 Ebon AZC	15 SiC Beta	1825 c				1.69	4.14	1502	83.3		109	5.1	
3-1	90 Ebon A	10 SiC UF-15	1600 c	3.813	3.91	97.5	.41	5.07/3.71	----	62.4	430.2	88	7.2	
3-2	70 A-16	30 SiC F-1000	1600 c	3.741	3.75	99.8	1.15	7.34	----	47.7	328.9	68	4.4	
3-3	90 A-16	10 SiC F-1000	1600 c	3.896	3.91	99.6	2.7	3.93	----	60.1	414.4	62	48.4	
3-6	55 Ebon AZC	45 SiC UF-15	1600 c	3.743	3.70	100	**	4.2	----	58.2	401.3	83	4.1	
3-7	70 Ebon AZC	30 SiC UF-15	1600 c	3.895	3.84	100	0.5	3.51	----	84.1	579.9	97	7.6	
3-8	90 Ebon AZC	10 SiC UF-15	1600 c	4.07	4.01	100	1.15	3.48	----	83.6	576.4	93	17.6	
4-1	90 A-16	10 SiC UF-15	1750 c	3.895	3.91	99.6	5.36	----	----	48.6	335.3	58.9	8.4	
4-2	80 A-16	20 SiC UF-15	1750 c	3.819	3.83	99.7	2.88	----	----	69.1	482.6	77.9	10.8	
4-3	90 A-16	10 SiC F-1000	1750 c	3.895	3.91	99.6	4.96	----	----	50.9	355.5	60.9	9.2	
4-4	70 A-16	30 SiC F-1000	1750 c	3.744	3.75	99.8	4.92	----	----	45.8	319.9	52.9	12.2	
4-5	50 A-16	50 SiC F-1000	1750 c	3.594	3.60	99.8	6.32	----	----	45.4	317.1	52.4	9.7	
	100 Ebon A			3.96	3.99	99.2	2.1	5.0	1450	98	620.6	----	9	
	100 Ebon AZC			4.08	4.11	100	.86	2.98	1545	86	593.7	97.7	7	
	PAD SiC Type B			3.19	3.23	98.8	2.2	5.8	----	90	620.6	----	18	

* K_{IC} results unattainable with technique used

** Grain Size not obtained, Material would not Etch

APPENDIX I

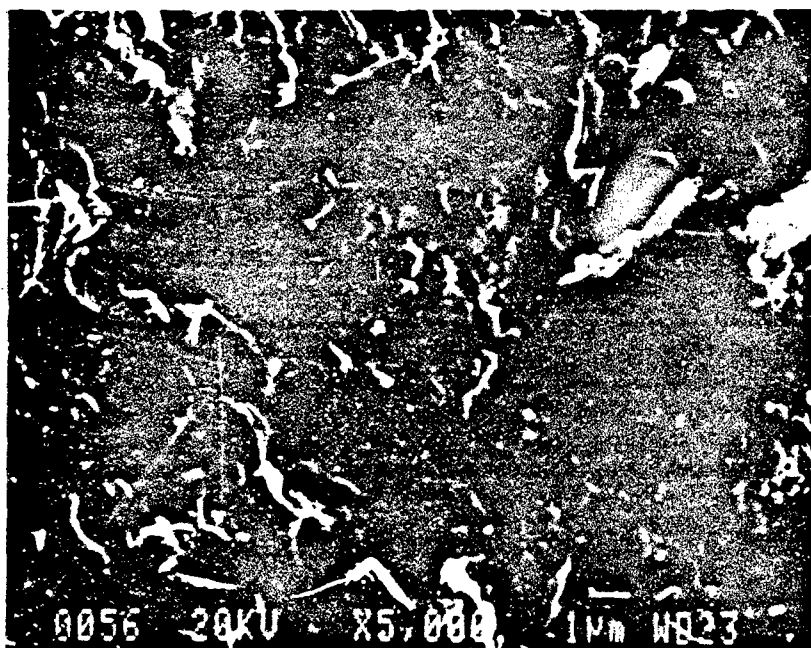


657-1

Al_2O_3

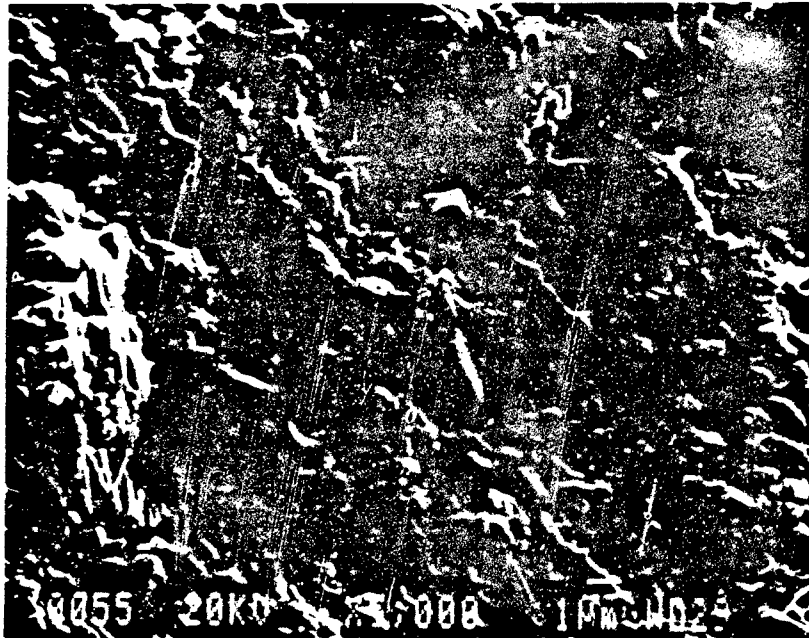
1600°C 3000 psi

Al_2O_3 Ceralox



657-2

Al_2O_3 • 10% SiC
 1600°C 3000 psi
 SiC HCS Beta
 Al_2O_3 Ceralox



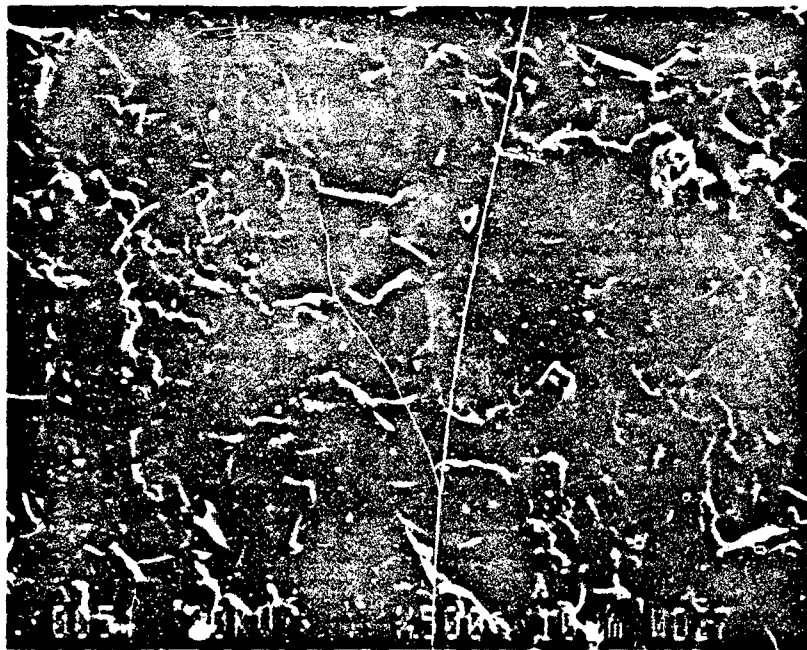
657-3

Al_2O_3 • 20% SiC

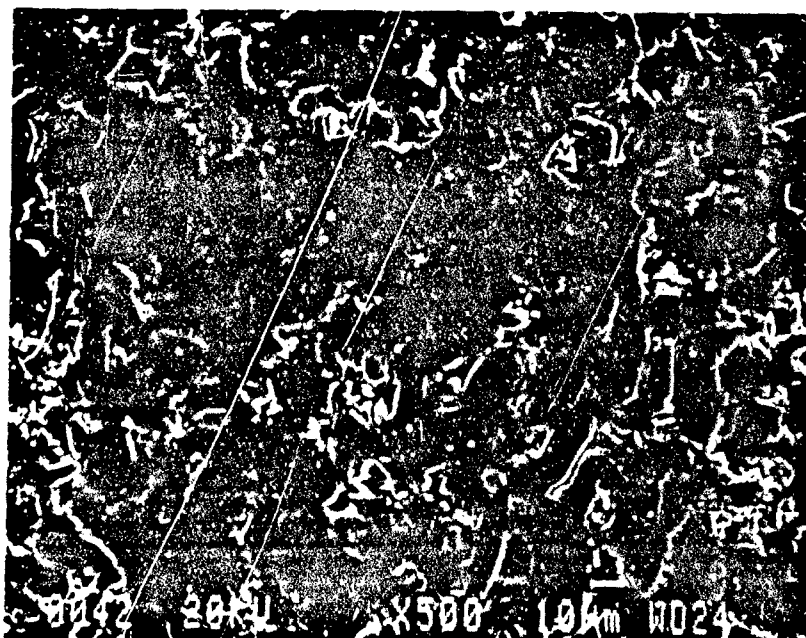
1600°C 3000 psi

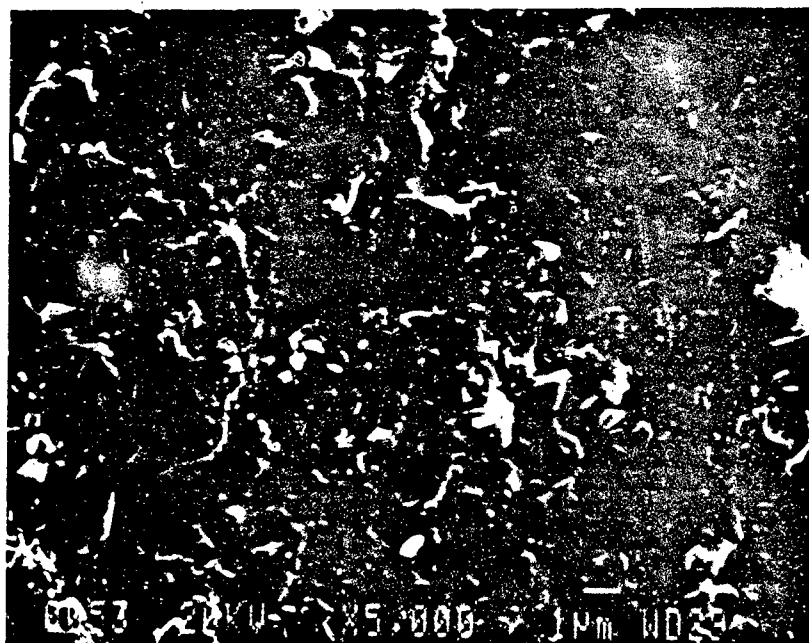
SiC HCS Beta

Al_2O_3 Ceralox



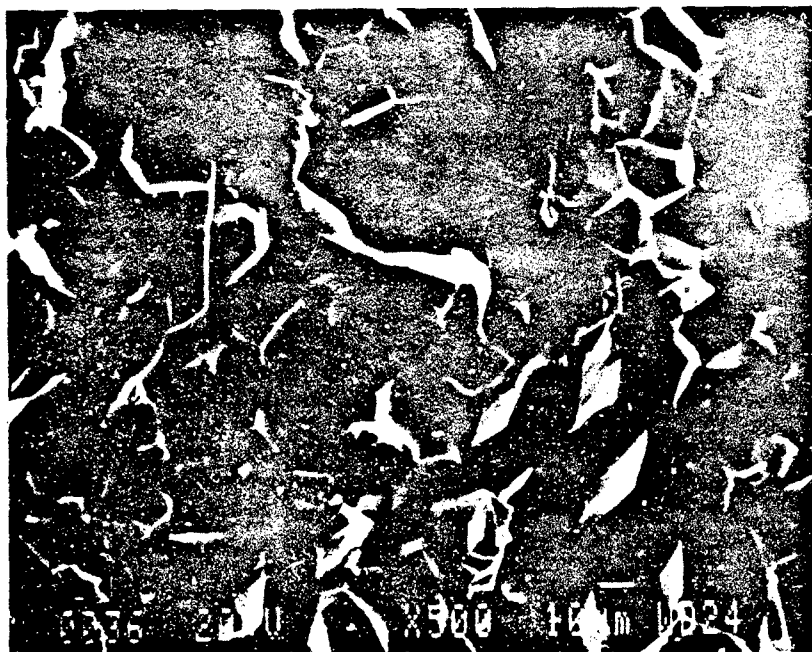
657-4
 Al_2O_3
 1600°C 3000 psi
 Al_2O_3 A-16



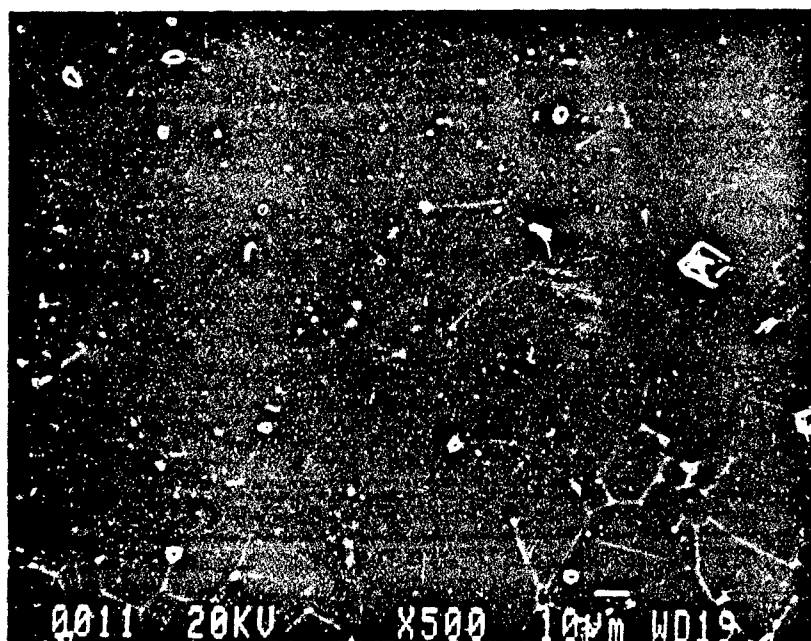


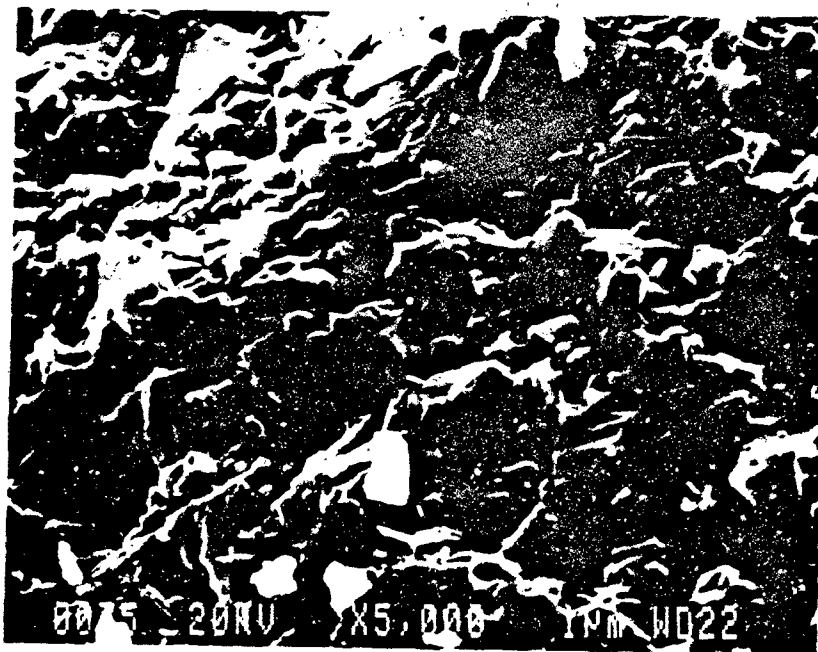
657-5

Al_2O_3 • 10% SiC
1600°C 3000 psi
 Al_2O_3 A-16
SiC 15 UF



660-3
 Al_2O_3
 1825°C 3000 psi
 Al_2O_3 A-16





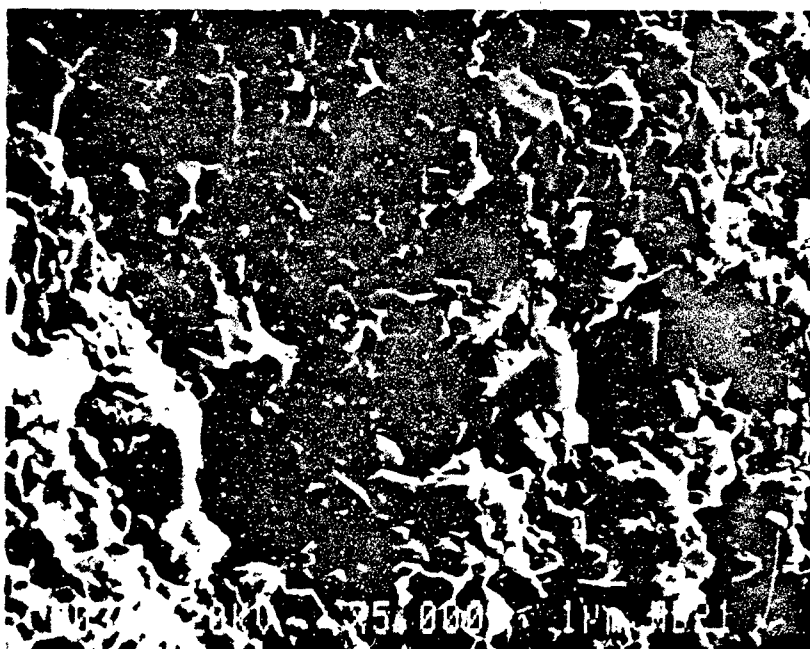
660-4

Al_2O_3 • 30% SiC

1825°C 3000 psi

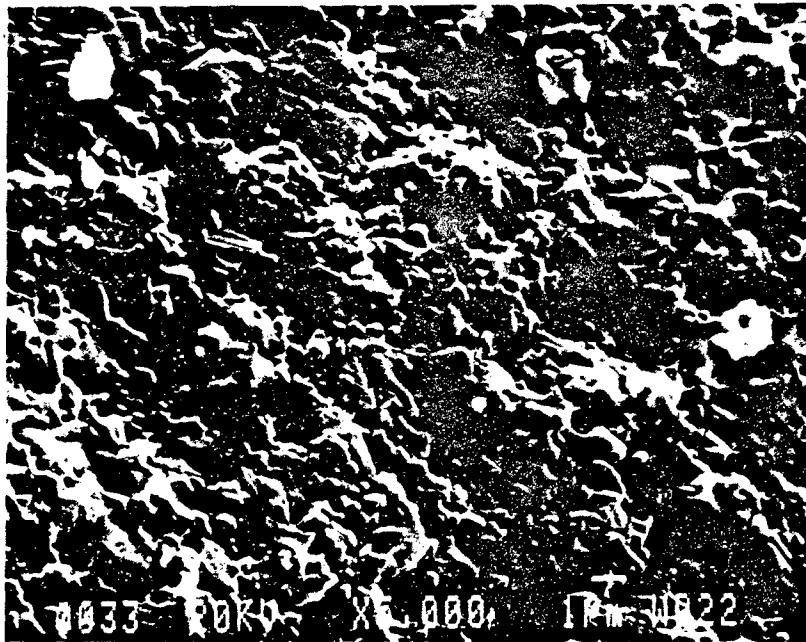
Al_2O_3 A-16

SiC HCS Beta



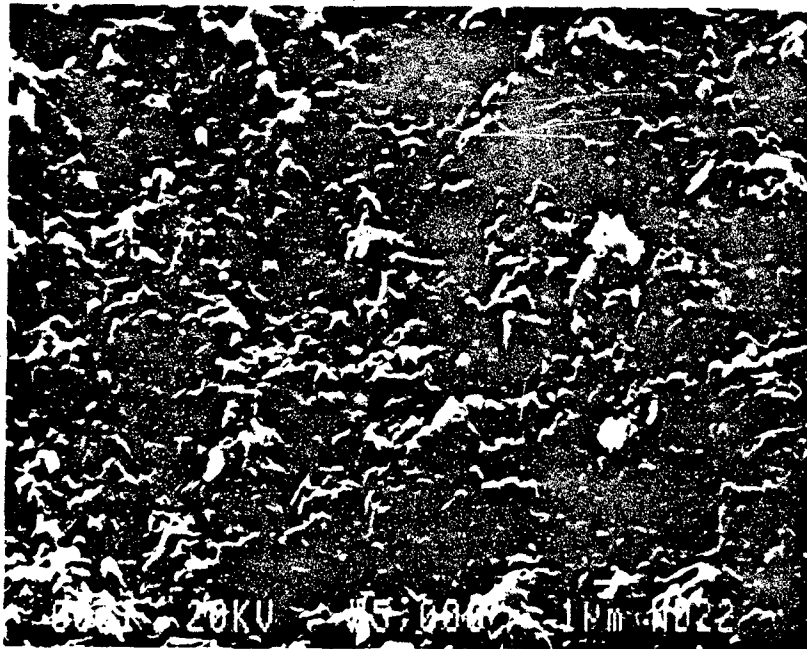
660-5

Al_2O_3 • 50% SiC
1825°C 3000 psi
 Al_2O_3 A-16
SiC HCS Beta



660-6

Al_2O_3	•	30% SiC
1825°C		3000 psi
Al_2O_3		A-16
SiC		15 UF



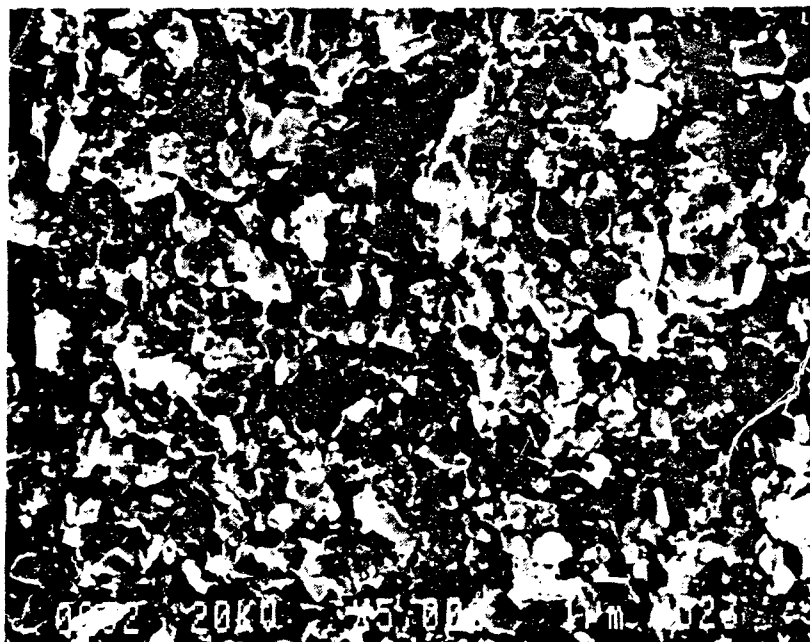
660-7A

Al_2O_3 • 50% SiC

1825°C 3000 psi

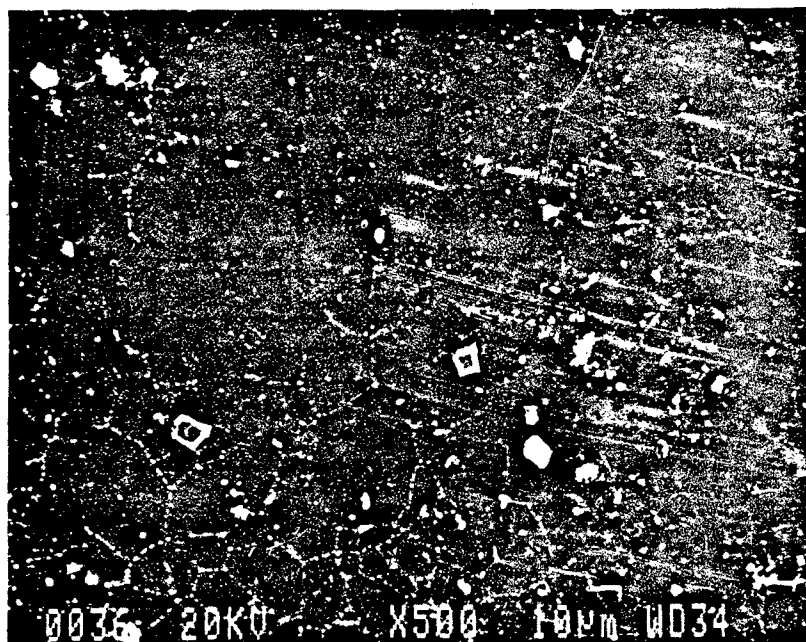
Al_2O_3 A-16

SiC 15 UF

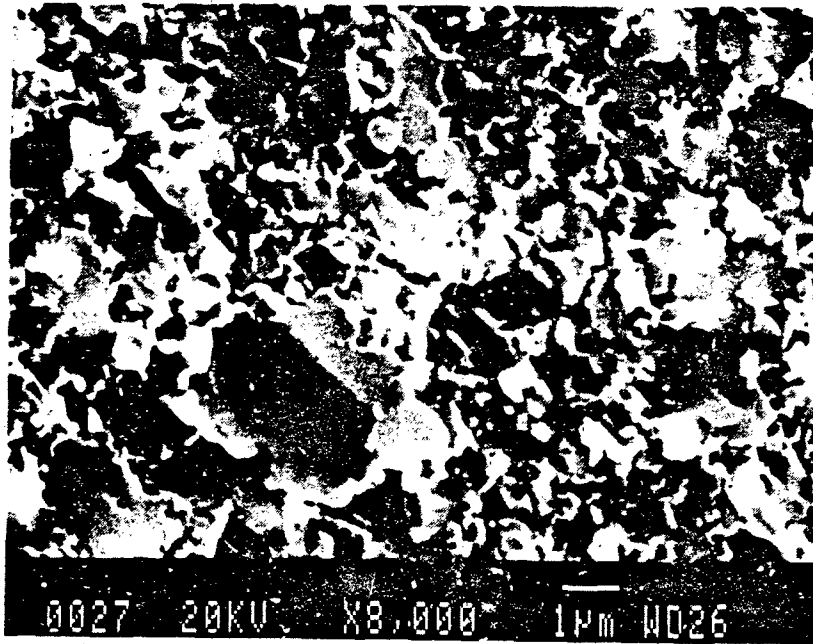


660-7B

Al_2O_3	•	50% SiC
1825°C		3000 psi
Al_2O_3		A-16
SiC		15 UF

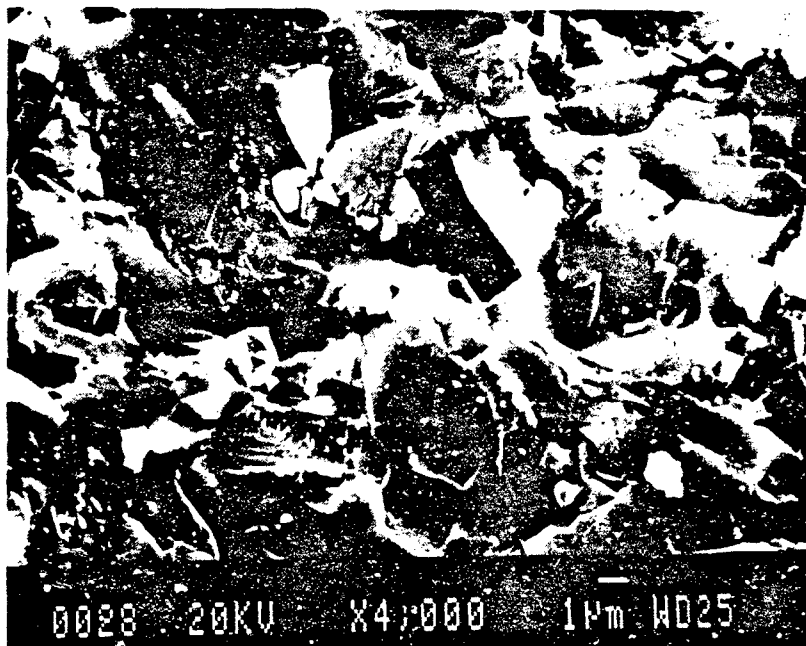


674-1
 Al_2O_3
1825°C 3000 psi
 Al_2O_3 Ceralox



763-1

Ebon A • 10% SiC
1600°C 3000 psi
SiC 15 UF



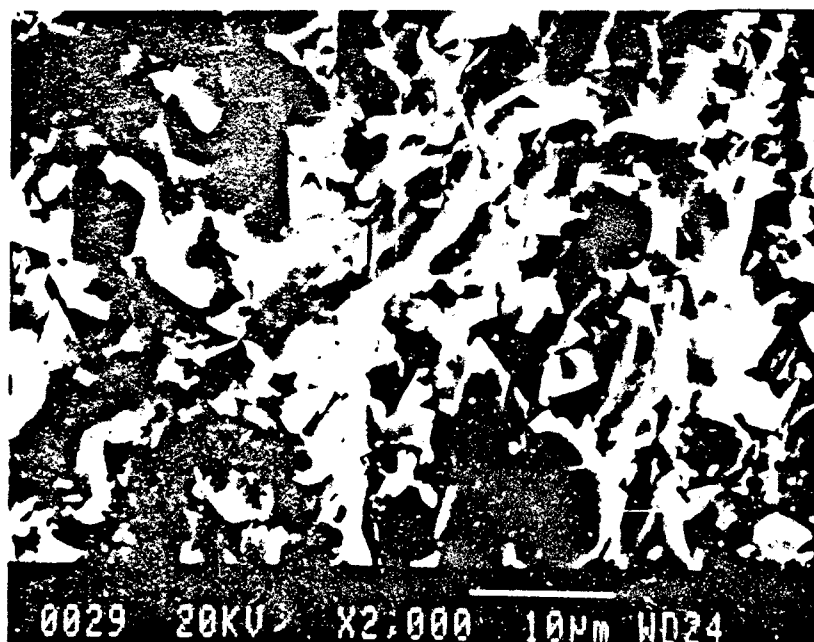
763-2

Al_2O_3 • 30% SiC

1600°C 3000 psi

Al_2O_3 A-16

SiC 1000 grit



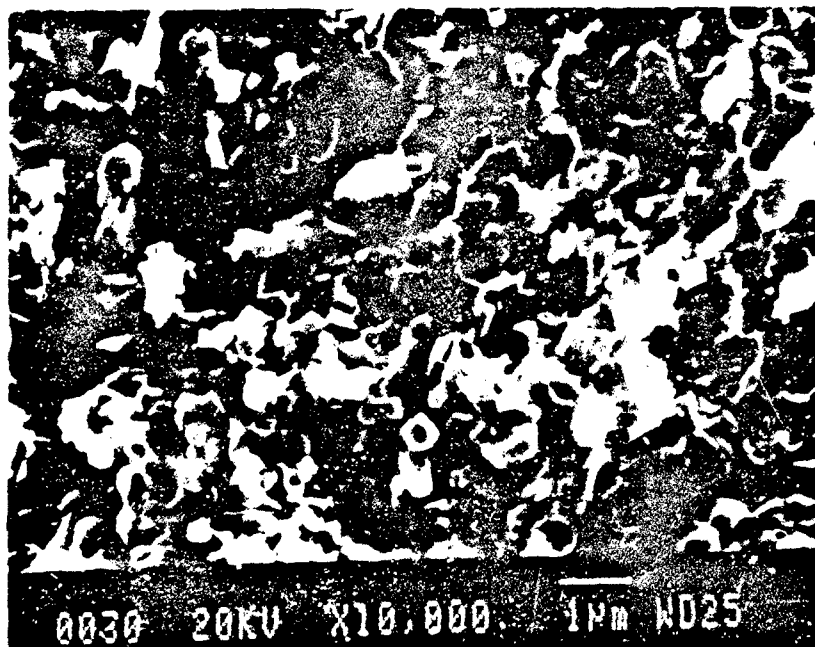
763-3

Al_2O_3 • 10% SiC

1600°C 3000 psi

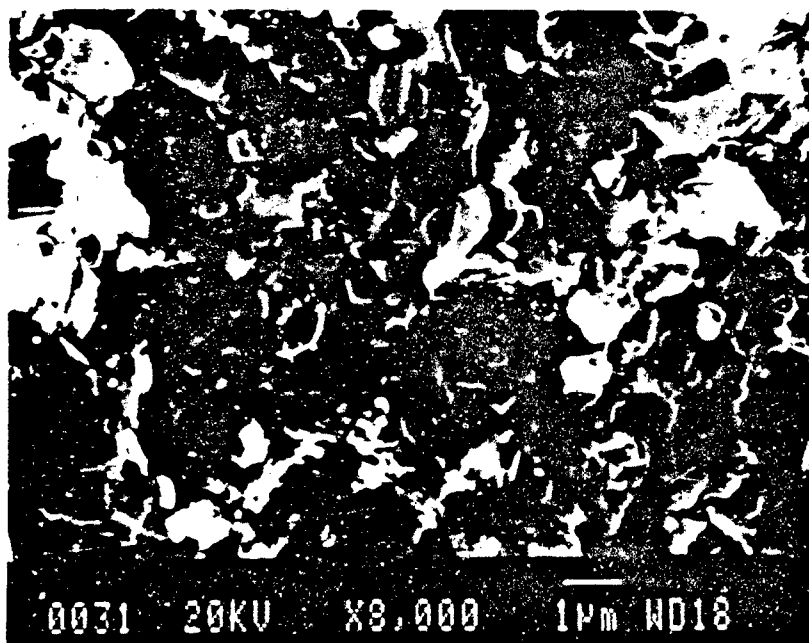
Al_2O_3 A-16

SiC 1000 grit



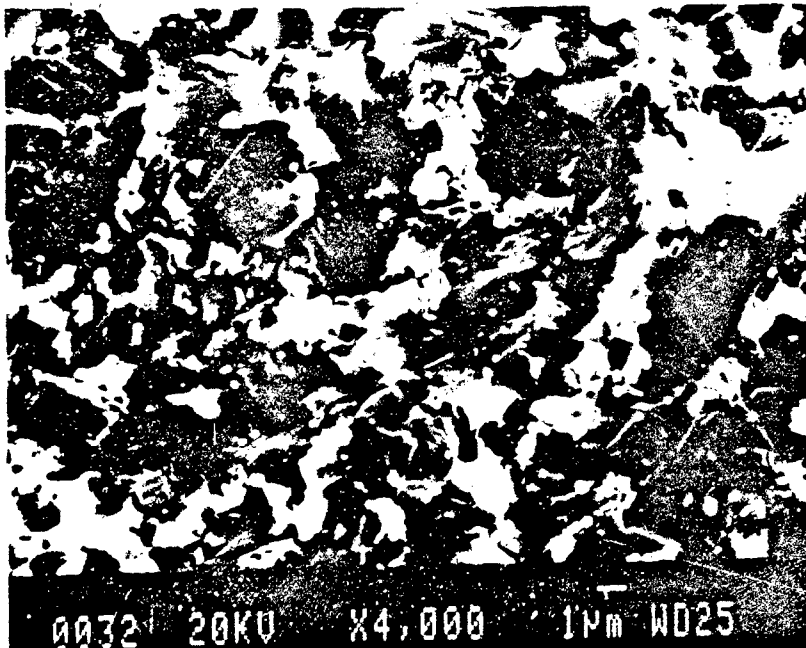
763-6

Ebon AZC • 45% SiC
1600°C 3000 psi
SiC 15 UF



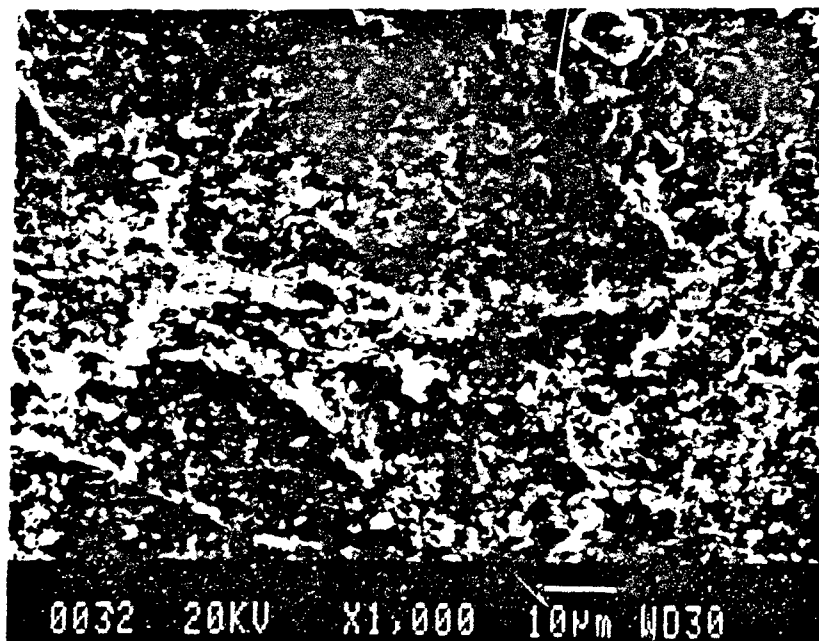
763-7

Ebon AZC • 30% SiC
1600°C 3000 psi
SiC 15 UF



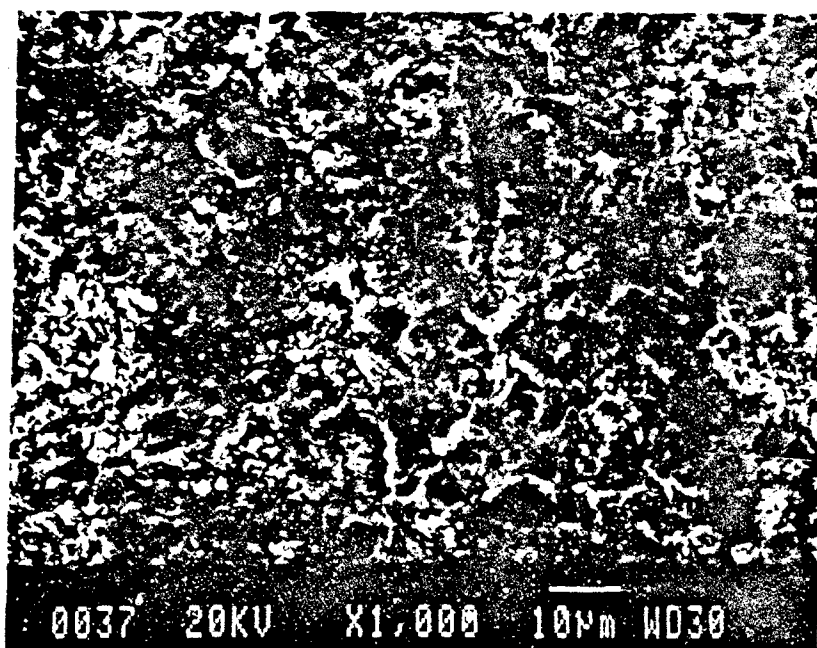
763-8

Ebon AZC ● 10% SiC
1600°C 3000 psi
SiC 15 UF



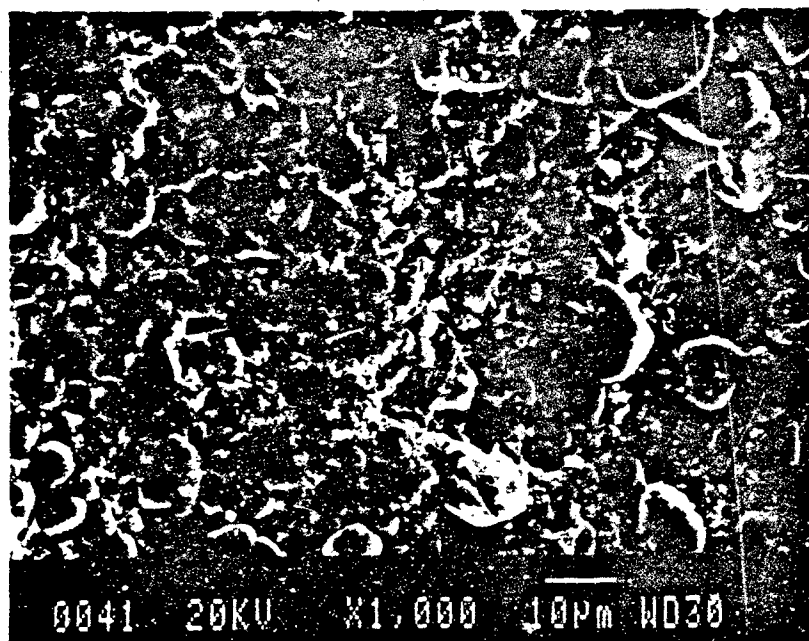
774-1

Al_2O_3 • 10% SiC
1750°C 3000 psi
SiC 15 UF
 Al_2O_3 A-16



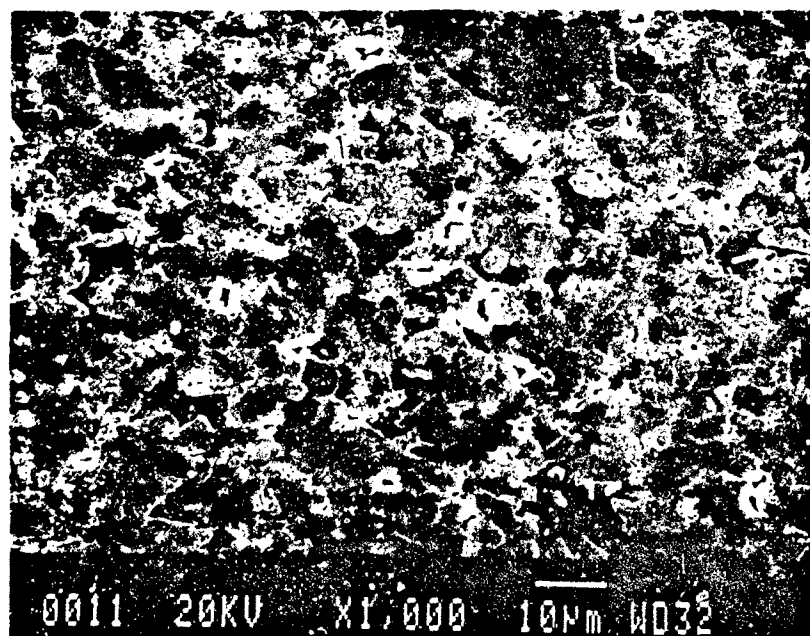
774-2

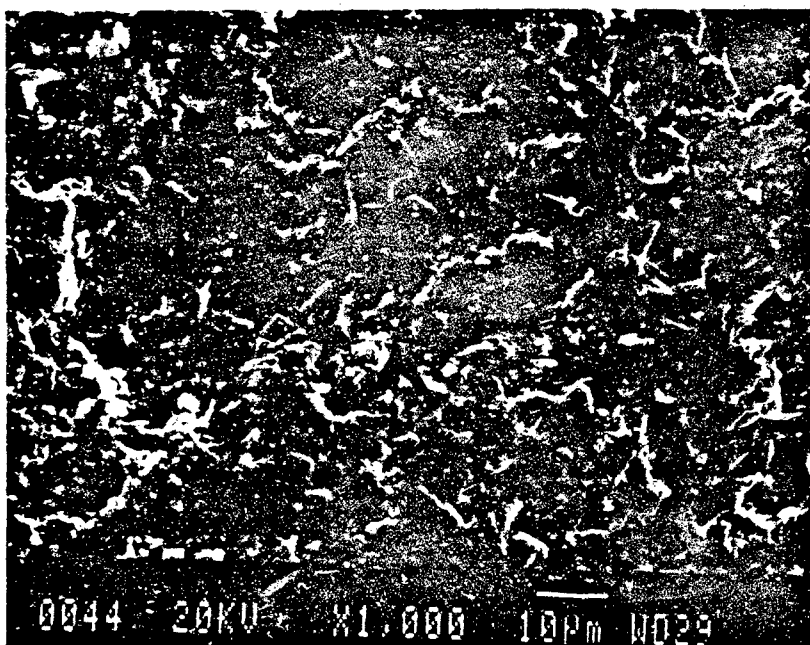
Al_2O_3 • 20% SiC
1750°C 3000 psi
SiC 15 UF
 Al_2O_3 A-16



774-3

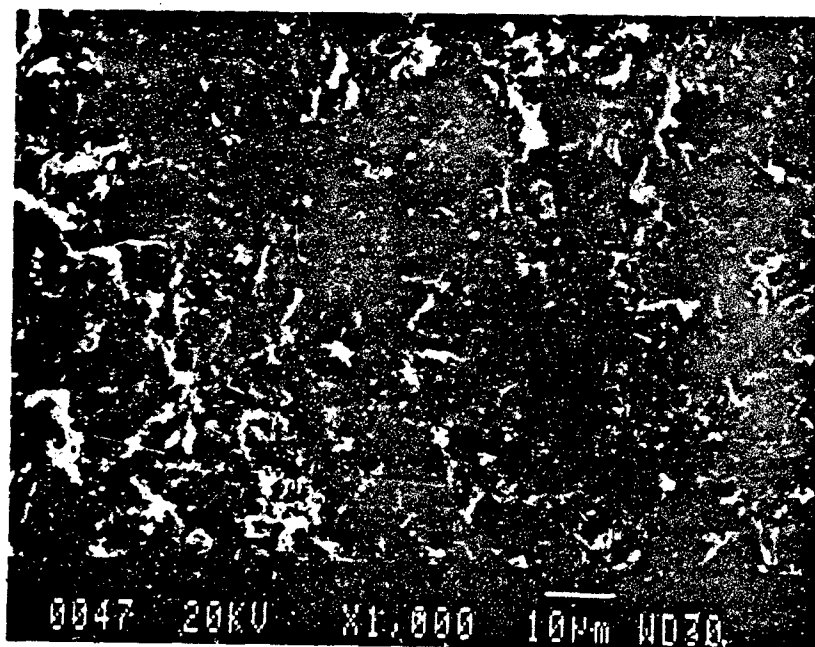
Al_2O_3 • 10% SiC
 1750°C 3000 psi
 SiC 1000 grit
 Al_2O_3 A-16





774-4

Al_2O_3 • 30% SiC
1750°C 3000 psi
SiC 1000 grit
 Al_2O_3 A-16

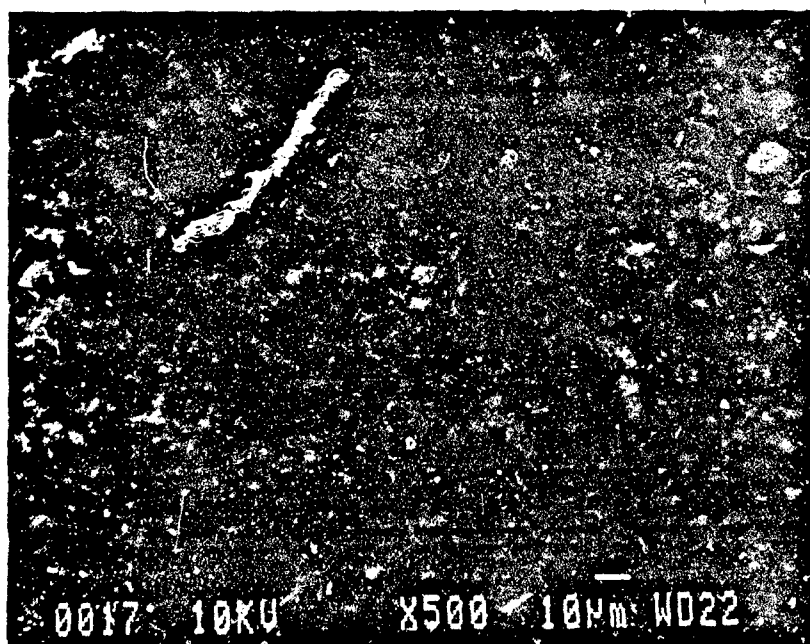


774-5

Al_2O_3 • 50% SiC
1750°C 3000 psi
SiC 1000 grit
 Al_2O_3 A-16



"PAD" SiC Type B



"PAD" SiC Type B

**END
FILMED**

DATE: 1-92

DTIC